70. PRELIMINARY LIPID ANALYSES OF SECTIONS 440A-7-6, 440B-3-5, 440B-8-4, 440B-68-2, AND 436-11-4: LEGS 56 AND 57, DEEP SEA DRILLING PROJECT

S. C. Brassell, P. A. Comet, G. Eglinton, P. J. Isaacson, J. McEvoy, J. R. Maxwell, I. D. Thomson, P. J. C. Tibbetts, and J. K. Volkman, Organic Geochemistry Unit, University of Bristol, School of Chemistry, Cantock's Close, Bristol BS8 1TS, England

ABSTRACT

"Bound" and "free" solvent-extractable lipids have been examined from Sections 440A-7-6, 440B-3-5, 440B-8-4, 440B-68-2, and 436-11-4. The compound classes studied include aliphatic and aromatic hydrocarbons, ketones, alcohols, and carboxylic acids. Carotenoids and humic acids have also been examined. The quantitative results are considered in terms of input indicators, diagenesis parameters, and structural classes. A difference in input is deduced across the Japan Trench, with a higher proportion of autochthonous components on the western inner trench slope compared with the more easterly, outer trench, wall and greater input in the early Pleistocene than in the Miocene. A variety of diagenetic transformations is observed at Site 440 as sample depth increases. Results are compared with those of samples from Atlantic Cretaceous sediments and from the Walvis Bay high productivity area.

INTRODUCTION

The compositions of lipid components have been investigated in selected sections from two sites (436 and 440) of the Japan Trench transect, drilled during Legs 56 and 57. Both "free" and "bound" lipids were obtained by extraction into organic solvents, the "bound" after acid treatment and alkaline hydrolysis of the sample. In the following, these fractions are termed simply free or bound. The compound classes examined include aliphatic and aromatic hydrocarbons, ketones, alcohols, carboxylic acids, and carotenoids. These were analyzed by various chromatographic, spectroscopic, and spectrometric methods. In addition, preliminary analyses of humic acids were performed.

This preliminary report describes the lipid composition of five samples and presents the data in tabular and figure form. The amount of data precludes detailed discussion of their significance here, but compounds (or ratios of compounds) which are indicative of inputs, and of the extent of diagenesis, are listed and the overall conclusions summarized. Comparisons are made with other sediments examined by us. Further samples from Legs 56 and 57 are under study, and detailed discussion of the combined results will be submitted elsewhere.

Table 1 summarizes the lithological characteristics of the core sections investigated and includes the sample weights. The samples thawed during shipment from Japan to the U.S. Following refreezing and delivery, they were stored at subzero temperature until extraction. Subsamples (approx. 5 g) were taken from the frozen core sections for visual kerogen and total organic carbon analyses by British Petroleum Ltd., Sunbury-on-Thames.

The experimental scheme used was similar to that of our previous DSDP investigations (Barnes et al., 1979; Brassell et al., in press) but differed in the scope of lipid classes examined.

EXPERIMENTAL PROCEDURES

General

The basic experimental scheme for samples and blank analyses performed in parallel is shown in Figure 1. It differs from our previous investigations (Barnes et al., 1979; Brassell et al., in press) in the following ways: (1) both free and bound lipids are examined, (2) humic acid analyses are performed, (3) a radical inhibitor is added to the appropriate fractions, (4) an aliquot (10 per cent) of the free neutrals is taken for carotenoid analysis, and (5) a subsample (approx. 30 per cent) was set aside for extraction, thereby permitting isolation of unaltered carotenoids. Details are given below:

1) Free lipids are designated as those extractable by the organic solvent system used. The residue was sonicated in HCl (*p*H 1). Saturated aq. KOH/MeOH (10 ml) and double-distilled water (100 ml) were added and the mixture heated under reflux overnight. Bound lipids are similarly extractable from the alkali hydrolysate of the acid-treated residue from the first extraction. Bound neutrals were extracted directly into CH_2Cl_2, and bound acids were similarly recovered following acidification to *p*H 1. Further separation of the bound fractions by TLC was not attempted. The same techniques were used for analysis of both bound and free fractions.

2) Humic acids (HAs) comprise the CH_2Cl_2-insoluble precipitate remaining after extraction of bound lipids. These were dialyzed against distilled water for 24 h,

TABLE 1
Samples from Holes 440A, 440B, and 436

Hole	Core	Section	Interval (cm)	Sub-bottom Depth (m)[a]	Age (m.y.B.P.)[a]	Lithology[a]	Dry Wt. (g)	Organic Carbon (%)[b]
440A	7	6	125–150	139	Lower Pleistocene (approx. 1)	Olive gray, firm, homogeneous, diatomaceous silty clay intercalated with patches of sponge fragments	50	1.05
440B	3	5	125–150	166	Lower Pleistocene (approx. 1)	Olive gray, firm, homogeneous, diatomaceous clay, slightly calcitic	48	1.0
440B	8	4	125–150	212	Lower Pleistocene (approx. 1)	Slightly streaked and mottled grayish olive diatomaceous clay/grayish olive silty claystone	97	0.5
440B	68	2	130–150	779	Upper Miocene (approx. 6)	Dark, greenish gray silty claystone	61	0.4
436	11	4	100–120	99	Pliocene (approx. 2)	Dusky yellowish green, moderately deformed diatomaceous vitric clay	65	0.35

[a]From site reports including data for Holes 440A, 440B, and 436, this volume, Pt. 1.
[b]Data obtained from subsample analysis by British Petroleum Co., Ltd.

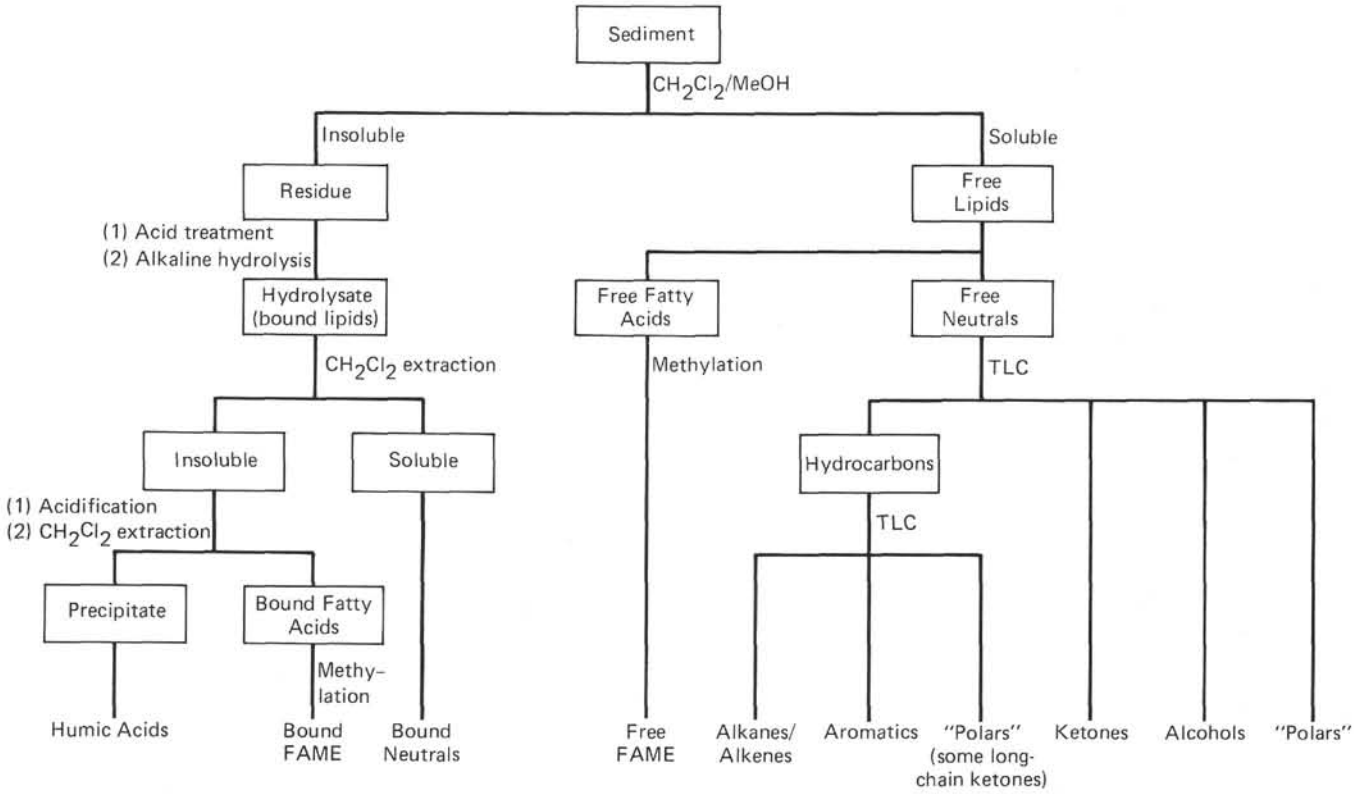

Figure 1. *Experimental scheme.*

then freeze-dried. Elemental analyses were performed for C, H, N, S, and O (by difference) and the inorganic residue weighed. Visible spectra were recorded for 0.01 per cent w/v solutions in 0.1 M KOH solution, using an SP 1800 Unicam spectrophotometer and 10-mm cells.

Infrared spectra were recorded on a Perkin Elmer 580 infrared spectrometer. HAs (2 mg) dispersed in predried KBr (300 mg) were pressed to pellet form. A blank pellet was run to check the absence of absorption due to moisture.

3) The radical inhibitor 2,6-di-t-butyl-4-methylphenol was added to the hydrocarbon fractions to stabilize certain compounds, e.g. diasterenes.

4) An aliquot (10 per cent v/v) of the free neutral fraction was examined by ultraviolet/visible (uv/vis) spectrophotometry and by HPLC. Both continuous and stopped-flow scans were recorded.

5) The subsample of 440A-7-6 was extracted in the usual manner and esterified (CH_2N_2). HPLC and uv/vis analyses of the total and fractionated materials are be-

ing performed to determine unaltered carotenoid distributions.

Precautions were taken at all stages to minimize contamination, as reported previously (Barnes et al., 1979) In particular, it was necessary to predevelop TLC plates exhaustively.

Gas chromatography (GC) was performed on a Carlo Erba 2150 gas chromatograph, equipped with a 20-m SE-52 glass capillary column (0.25-mm inside diameter) and He as carrier gas. The instrument was temperature programmed at 4°C min.$^{-1}$ from 50–275°C, followed by up to 30 min. isothermal running. Further analyses of chosen fractions were carried out on a 12-m OV-1 glass capillary column (100–280°C at 4°C min.$^{-1}$).

Mass spectra were recorded using a Finnigan 4000 gas chromatograph–mass spectrometer (GC–MS) system equipped with either 20-m or 12-m OV-1 WCOT glass capillary columns. Data acquisition and processing were performed by a PDP 8e computer. Typical operating conditions were ion source temperature 250°C, electron energy 35 eV, and filament current 350 μA.

The HPLC equipment used has been previously described (Brassell et al., in press). For carotenoid analysis, eluant absorbance was monitored at 451 nm, with the uv/vis spectra of individual peaks absorbing at this wavelength recorded by stopped-flow scanning. An acetone:hexane gradient system was programmed to change quadratically from 2:98 to 75:25 over 30 min.

RESULTS

General

All samples were free of visible pipe dope contamination. The blank analyses performed in parallel with the samples did not contain significant amounts of lipid except for squalene, which is presumed to come from the TLC plates.

Structural assignments were based on (1) GC retention times, (2) comparison of mass spectra with those of authentic standards (where available), or literature spectra, (3) spectral interpretation, or (4) mass fragmentography (MF) of diagnostic ions for homologous or pseudohomologous series. GC coinjections were performed when possible, particularly for aromatic hydrocarbons and the very long chain ketones. Quantitations were made by measurement of GC or MF peak areas and comparison with the response of components of known quantity. A major difficulty hindering accurate quantitation was the presence of some compounds (e.g., very long chain ketones in Section 440B-8-4) in more than one fraction after TLC separations.

Other errors inherent in the quantitation arise from measurements of peak areas and GC injection volumes, fluctuations in instrument sensitivity, and spectrum skewing in GC–MS analyses. The last phenomenon, which creates mass spectral distortion, occurs when the mass spectrometer scan rate is of the same order of magnitude as the GC peak width. Quantitation from MF will be particularly affected by spectrum skewing, introducing underestimations of perhaps 20 per cent for individual components. In general, quantitation of an individual class of compound is internally consistent, but comparison of the concentrations of different classes may not give a true representation of their relative amounts. Indeed, without the use of an internal standard for each compound class, such accuracy is difficult to achieve.

The results for each compound class are described individually in the following.

Aliphatic Hydrocarbons

Normal

The major class of hydrocarbon in all five samples is *n*-alkane, dominated by *n*-C_{29} (Figure 2). The amount of *n*-C_{24} in Section 436-11-4 is anomalously high, probably because of contamination from the *n*-C_{24} used as a standard in the preliminary separation of free neutral lipids by TLC. The carbon preference indices (CPI) for selected carbon number ranges are given in Table 2.

The odd-numbered *n*-alkanes in the range C_{23} to C_{35} dominate, with their dominance least marked in Section 440B-68-2. The amounts of C_{15} to C_{21} *n*-alkanes are lower relative to *n*-C_{29} in Section 436-11-4 than in the samples from Site 440, particularly Section 440B-68-2. The total amounts of *n*-alkanes in Sections 440A-7-6 and 440B-3-5 are similar and higher than those of Sections 440B-8-4, 440B-68-2, and 436-11-4. Sections 440A-7-6, 440B-3-5, and 440B-8-4 closely resemble one another in their distributions.

The distributions showed no obvious signs of contamination from pipe dope or other shipboard sources. The presence of a "hump" in the alkane/alkene fraction of Sections 440B-8-4 and 440B-68-2 did, however, suggest that these particular samples might contain minor contributions from shipboard oil-based contaminants.

MF searches of m/e 83 showed that *n*-alkenes were not present in any of the samples.

Branched/Cyclic

No significant amounts of simple branched alkanes or alkenes, such as 7-methylheptadecane, were detected in any of the samples by MF searches (e.g., of m/e 85).

The concentrations of acyclic isoprenoid alkanes and alkenes are given in Table 3. The pristane-to-phytane ratio of each sample is also shown. Each component was recognized from its mass spectrum and GC retention time.

The relative amounts of pristane and phytane are markedly lower in Section 436-11-4 than in the other samples, whereas the content of 2,6,10,15,19-pentamethyleicosane (I) and squalane (II) are similar. Section 440B-8-4 is the only sample that contains a higher proportion of the C_{25} isoprenoid alkane than squalane. Sections 440A-7-6 and 440B-3-5 possess similar isoprenoid alkane distributions, and both contain greater proportions of pristane and phytane than of C_{25} and C_{30} isoprenoids, unlike the other sections, in which one or both of the latter components predominate.

The pristane to phytane ratio shows no definite trend with depth at Site 440.

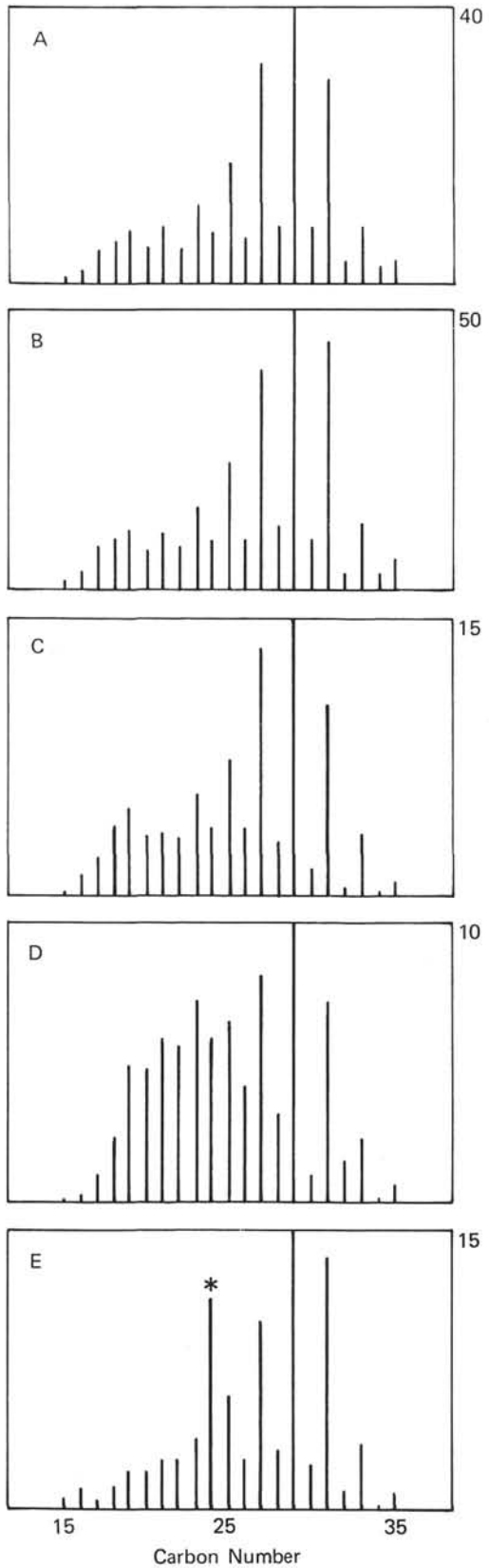

Figure 2. *Abundance (ng/g dry sediment) of* n-*alkanes from C_{15} to C_{35}.* A. *Section 440A-7-6;* B. *Section 440B-3-5;* C. *Section 440B-8-4;* D. *Section 440B-68-2;* E. *Section 436-11-4. (* = n-C_{24} contamination from TLC standard.)*

TABLE 2
Normal Alkane Carbon Preference Indices

	Carbon Number Range		
Section	15–21	22–35	15–35
440A-7-6	1.22	3.40	2.69
440B-3-5	1.16	3.74	2.53
440B-8-4	0.94	3.54	2.50
440B-68-2	1.21	1.96	1.70
436-11-4	0.94	3.66[a]	2.84[a]

[a]True n-C_{24} concentration assumed equal to n-C_{22}, to minimize distortion due to contamination (see text).

TABLE 3
Abundance of Acyclic Isoprenoid Alkanes/Alkenes (ng/g dry sediment)

	Section				
Component	440A-7-6	440B-3-5	440B-8-4	440B-68-2	436-11-4
pristane	4.2	6.2	0.5	0.8	0.3
phytane	3.5	4.9	1.0	0.9	0.4
phytene[a]	0.7	0.8	Tr	Tr	n.d.
phytene[a]	6.5	6.0	0.2	0.1	n.d.
phytene[a]	9.7	10.7	0.4	0.3	n.d.
2,6,10,15,19-pentamethyleicosane	1.5	1.9	1.7	1.4	0.3
squalane	2.8	3.1	0.9	1.7	0.6
pristane/phytane ratio[b]	1.2	1.2	0.49	0.85	0.77

Note: Tr = trace amounts of compound (<0.1 ng/g dry wt. sediment), n.d. = not detected.
[a]phytene isomers, double bond position not assigned.
[b]pristane/phytane ratio calculated directly from GC response.

The quantity of phytenes is considerably greater in the upper two sections of Site 440 than in the lower two samples, with the major isomers more abundant than pristane or phytane. The amounts of the individual phytene isomers in Sections 440B-8-4 and 440B-68-2 are too small to determine whether there is a trend in the relative proportions of each isomer with increasing depth. No phytenes were detected in Section 436-11-4.

Steranes were identified in similar concentrations and distributions in Sections 440B-8-4 and 440B-68-2 by mass spectral interpretation and from MF of m/e 217 (Table 4). Steranes were present in only trace quantities in the shallower Site 440 samples and were not detected in Section 436-11-4. The 5α configuration was assigned for a series of C_{27} to C_{29} components on the basis of the m/e 149-to-m/e 151 ratio and GC retention times. A second unknown series of C_{27} to C_{29} steranes, eluting before their 5α counterparts, was observed.

4-methyl steranes were not detected by MF (m/e 231) in any of the samples. Neither diasteranes nor 4-methyl diasteranes were detected in any of the sections by MF searches of m/e 259 and m/e 273, respectively.

The major sterenes (mono-, di-, tri- and tetraunsaturated) were identified by mass spectral comparison with authentic standards or by spectral interpretation. In addition, MF of diagnostic ions (m/e 213, 215, 255,

TABLE 4
Concentration of Steranes (ng/g sediment)

Compound	Structure[a] R	Section 440B-8-4	Section 440B-68-2
C_{27}-sterane	III, H[b]	0.2	0.2
5α-cholestane	III, H	0.4	0.2
C_{28}-sterane	III, CH_3[b]	0.3	0.2
24-methyl-5α-cholestane	III, CH_3	0.3	0.2
C_{29}-sterane	III, C_2H_5[b]	0.2	0.2
24-ethyl-5α-cholestane	III, C_2H_5	0.4	0.4

[a] General structures; individual peaks not assigned to this or any other isomer.
[b] Unknown series.

and 257) was used for comparison and quantitation. Sterenes are relatively minor constituents of all Site 440 sections (Table 5; Figure 3). Only trace quantities of sterenes were detected in Section 436-11-4.

The sterene distributions in Sections 440A-7-6 and 440B-3-5 are similar and possess markedly greater proportions of tetra- and triunsaturated sterenes relative to Sections 440B-8-4 and 440B-68-2. The overall concentrations of sterenes in the two deeper sections are considerably lower than in the two shallower samples (Figure 3). The major component in three of them is a Δ^{22}-24-methylcholestatriene with two nuclear double bonds. No 4-methyl sterenes were detected in any of the samples by MF (especially m/e 229).

A series of diasterenes (rearranged sterenes) was assigned in all Site 440 sections by MF of m/e 257 and comparison with Leg 50 sample data (Brassell et al., in press). The concentrations, calculated from MF (m/e 257), are given in Table 6. No diasterenes were detected in Section 436-11-4.

TABLE 5
Concentration of Sterenes (ng/g dry sediment)[a]

Compound[b]	Formula	Structure[c] R	Section 440A-7-6	440B-3-5	440B-8-4	440B-68-2
1. C_{27} 3Δ (mixed)	$C_{27}H_{42}$	IV, H	0.4	0.2	Tr	n.d.
2. C_{27} $2\Delta^N$, Δ^{SC}	$C_{27}H_{42}$	IV, H	0.4	0.5	0.2	Tr
3. C_{27} Δ^2	$C_{27}H_{46}$	IV, H	0.8	0.8	0.1	0.1
4. C_{27} $\Delta^{3,5}$	$C_{27}H_{44}$	IV, H	0.7	0.9	0.3	0.2
5. C_{28} $2\Delta^N$, Δ^{22}	$C_{28}H_{44}$	IV, CH_3	1.7	2.1	0.4	0.3
6. C_{28} $2\Delta^N$, $\Delta^{24(28)}$	$C_{28}H_{44}$	IV, CH_3	1.2	1.6	0.8	Tr
7. C_{28} Δ^2	$C_{28}H_{48}$	IV, CH_3	0.6	0.9	0.2	Tr
8. C_{28} Δ^N, $\Delta^{24(28)}$	$C_{28}H_{46}$	IV, CH_3	1.2	1.2	Tr	Tr
9. C_{28} 4Δ	$C_{28}H_{42}$	IV, CH_3	0.9	0.5	n.d.	n.d.
10. C_{28} $2\Delta^N$, $\Delta^{24(28)}$	$C_{28}H_{44}$	IV, CH_3	1.5	1.3	Tr	Tr
11. C_{28} $\Delta^{3,5}$	$C_{28}H_{46}$	IV, CH_3	0.2	0.3	0.1	Tr
12. C_{29} $2\Delta^N$, $\Delta^{24(28)}$	$C_{29}H_{46}$	IV, C_2H_5	0.2	0.3	Tr	Tr
13. C_{29} $2\Delta^N$	$C_{29}H_{48}$	IV, C_2H_5	0.3	0.5	Tr	Tr
14. C_{29} Δ^2	$C_{29}H_{50}$	IV, C_2H_5	0.7	0.8	0.4	Tr
15. C_{29} $\Delta^{3,5}$	$C_{29}H_{48}$	IV, C_2H_5	0.6	0.8	0.2	0.2

Note: For explanation of Tr and n.d., see Note to Table 3.
[a] Quantitated from MF of diagnostic ions.
[b] First number refers to histogram bar, Figure 3. Nomenclature: double bond positions assigned where possible. Otherwise, Δ^N and Δ^{SC} indicate double bonds in nucleus or side chain, respectively (see IV).
[c] See Appendix, this chapter.

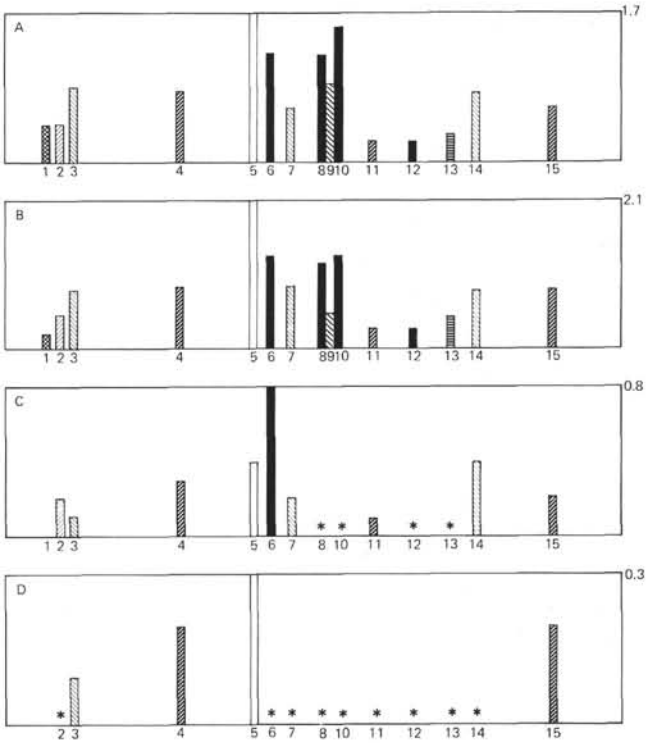

Figure 3. *Abundance (ng/g dry sediment) of sterenes.* A. *Section 440A-7-6;* B. *Section 440B-3-5;* C. *Section 440B-8-4;* D. *Section 440B-68-2. (Bar numbers refer to Table 5; * = presence in trace amount [< 0.1 ng/g] only.)*

TABLE 6
Concentration of Rearranged Sterenes (ng/g dry sediment)[a]

Formula	Structure,[b] R	Molecular Weight	Section 440A-7-6	440B-3-5	440B-8-4	440B-68-2
$C_{27}H_{46}$	V, H	370	n.d.	Tr	n.d.	Tr
$C_{27}H_{46}$	V, H	370	Tr	0.1	Tr	0.1
$C_{27}H_{46}$	V, H	370	n.d.	0.1	Tr	Tr
$C_{27}H_{46}$	V, H	370	0.1	0.4	0.1	0.2
$C_{28}H_{48}$	V, CH_3	384	0.1	0.2	Tr	0.2
$C_{28}H_{48}$	V, CH_3	384	n.d.	0.1	Tr	0.1
$C_{28}H_{48}$	V, CH_3	384	Tr	0.1	Tr	0.1
$C_{29}H_{50}$	V, C_2H_5	398	0.1	0.4	0.1	0.3
$C_{28}H_{48}$	V, CH_3	384				
$C_{28}H_{48}$	V, CH_3	384	n.d.	0.1	Tr	0.1
$C_{29}H_{50}$	V, C_2H_5	398	0.2	0.2	0.1	0.2
$C_{29}H_{50}$	V, C_2H_5	398	0.2	0.7	0.2	0.4
$C_{29}H_{50}$	V, C_2H_5	398	Tr	Tr	Tr	0.1

Note: For explanation of Tr and n.d. see Note to Table 3.
[a] ng/g dry wt. sediment, quantitated from MF of m/e 257.
[b] General structure; C-20 stereochemistry not determined (see Appendix, this chapter).

Section 440B-3-5 possesses the highest concentration of diasterenes, whereas Section 440B-68-2 is the only sample in which diasterenes are present in higher concentrations than sterenes.

MF of m/e 271, diagnostic of 4-methyl diasterenes, suggested that trace quantities were present only in Section 440B-68-2. No full spectra of these components were obtained and their assignment remains tentative.

Figure 4 shows the distribution of the major hopanes and hopenes (VI, VII, and VIII) recognized from their spectra, MF of key ions (m/e 191, m/e 189, m/e 177, m/e 205, m/e 231, and molecular ions), and GC retention characteristics. In addition to these, several minor components were observed by MF (particularly m/e 191). These included other C_{30} triterpenes (M^{+} 410) which were not fernenes (see the following), adianenes, or filicenes.

The major differences between the samples are as follows: (1) Section 436-11-4 contains a smaller proportion of hopenes (relative to hopanes) than Site 440; (2) the relative amounts of C_{30} and C_{31} 17βH, 21αH-hopanes (Figure 4, numbers 6 and 10, respectively) increase with increasing depth at Site 440; (3) there are smaller proportions of both C_{30} Δ^{21} and $\Delta^{22(29)}$ hopenes (Figure 4, numbers 13 and 12, respectively) in the lower two sections of Site 440 compared to the upper two (440A-7-6 and 440B-3-5); and (4) the proportion of C_{27} components [17βH-22,29,30-trisnorhopane and 22,29-30-trisnorhop-17(21)-ene; Figure 4, numbers 2 and 1, respectively] increases with increasing sediment depth.

Four fernene isomers were recognized from their characteristic m/e 243 fragmentation in individual mass spectra and quantified by MF. Their distribution and Kovat's indices are given in Table 7. The relative amounts of the individual fernene isomers show a definite trend with increasing depth, possibly reflecting a gradual diagenetic isomerization.

In addition to the recognized branched/cyclic components, three isomers of an unknown compound (M^{+} 326, $C_{24}H_{38}$) were detected in all samples. These compounds possessed some mass spectral characteristics common to those of the unknown $C_{24}H_{38}$ components present in algal mats from Laguna Guerrero Negro, Mexico (Philp et al., 1978), but were not identical.

Aromatic Hydrocarbons

A wide range of unsubstituted and alkyl-substituted polynuclear aromatic hydrocarbons (PAH) was detected in all samples, including several partially aromatic diterpenoid and triterpenoid derivatives. Identifications were made from individual mass spectra, MF of diagnostic ions, GC retention times, and, where possible, by coinjection with authentic standards. The components were quantified by their GC responses or from MF of diagnostic, usually molecular, ions. The results are given in Figure 5 and Table 8.

Perylene is the major component of all five samples and is especially dominant at Site 440. Its concentration (in ng/g dry sediment) ranges from 113 (Section 440A-7-6) to 31 (Section 440B-68-2) at Site 440, compared with 9.2 for Section 436-11-4. The ratio of perylene to total PAH is much lower in Section 436-11-4 than for any of the Site 440 sections. The homologous series of alkyl-substituted PAH tends to be present in greater concentrations than their respective unsubstituted arenes (Figure 5). At Site 440 the concentrations of phenanthrene (X, H) and the methylphenanthrene isomers (X, CH_3) tend to decrease with increasing depth, whereas the higher alkyl-homologues (i.e.,

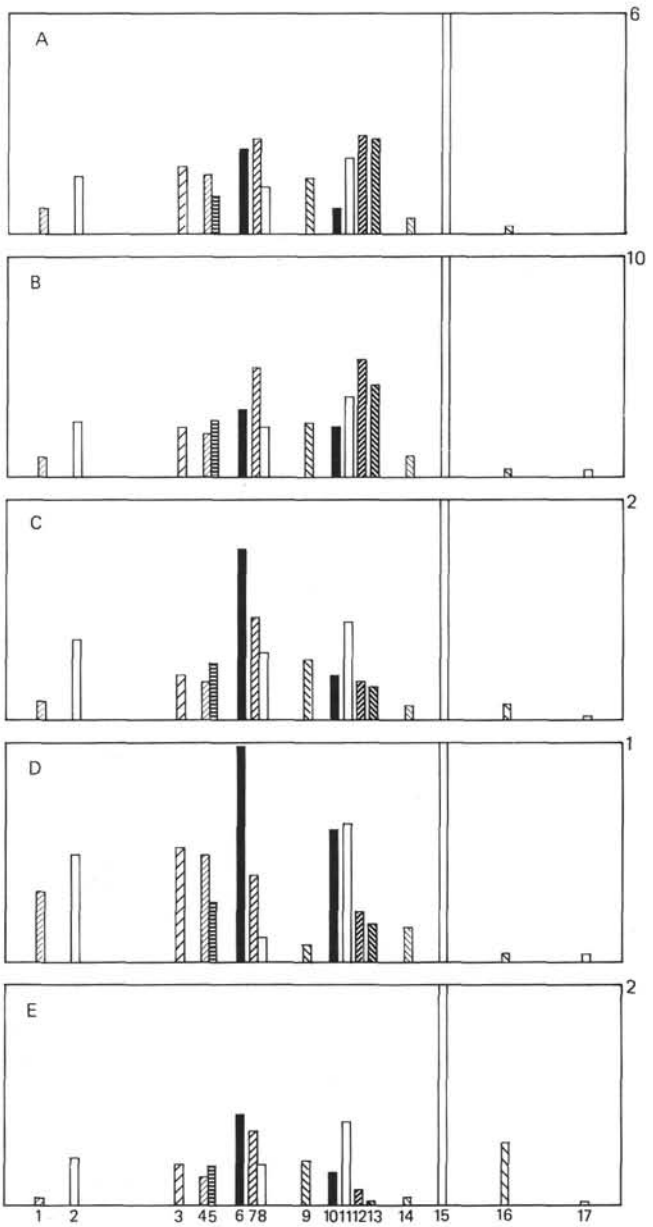

Figure 4. *Abundance (ng/g dry sediment) of major triterpanes/triterpenes.* A. *Section 440A-7-6;* B. *Section 440B-3-5;* C. *Section 440B-8-4;* D. *Section 440B-68-2;* E. *Section 436-11-4. Bar numbers correspond as follows: 1. 22,29,30-trisnorhop-17(21)-ene (VII, R:H); 2. 17βH-22,29,30-trisnorhopane (VI, R:H); 3. unknown C_{30} triterpene?; 4. hop-17(21)-ene (VII, R:CH(CH$_3$)$_2$); 5. 17β,21αH-30-norhopane (VI, R:C$_2$H$_5$; 6. 17αH,21βH-hopane (VI, R:CH(CH$_3$)$_2$); 7. neohop-13(18)-ene (VIII, $\Delta^{13(18)}$); 8. 17βH,21βH-30-norhopane (VI, R:C$_2$H$_5$); 9. neohop-12-ene (VIII, Δ^{12}); 10. 17αH,21βH-homohopane (VI, R:CH(CH$_3$)C$_2$H$_5$); 11. 17βH,21βH-hopane (VI, R:CH(CH$_3$)$_2$); 12. hop-22(29)-ene (VI, R:C(CH$_3$)=CH$_2$); 13. hop-21-ene (VI, R:=C(CH$_3$)$_2$); 14. homohop-30(31)-ene (VI, R:CH(CH$_3$)CH=CH$_2$); 15. 17βH,21βH-homohopane (VI, R:CH(CH$_3$)C$_2$H$_5$); 16. unknown C_{32} hopene?; 17. 17βH,21βH-bishomohopane (VI, R:CH(CH$_3$)CH$_2$C$_2$H$_5$).*

TABLE 7
Fernene Concentrations (ng/g dry sediment)[a]

Component[b]	Kovat's Index (OV-1)	Section 440A-7-6	440B-3-5	440B-8-4	440B-68-2	436-11-4
Fernene 1	2985	0.7	0.5	0.1	Tr	Tr
Fernene 2	3040	0.3	0.6	0.3	0.1	Tr
Fernene 3	3068	0.9	1.6	1.0	0.2	0.2
Fernene 4	3125	2.7	3.2	1.7	0.1	0.4

Note: For explanation of Tr see Note to Table 3.
[a]Quantitated from MF of m/e 243.
[b]Individual isomers not assigned.

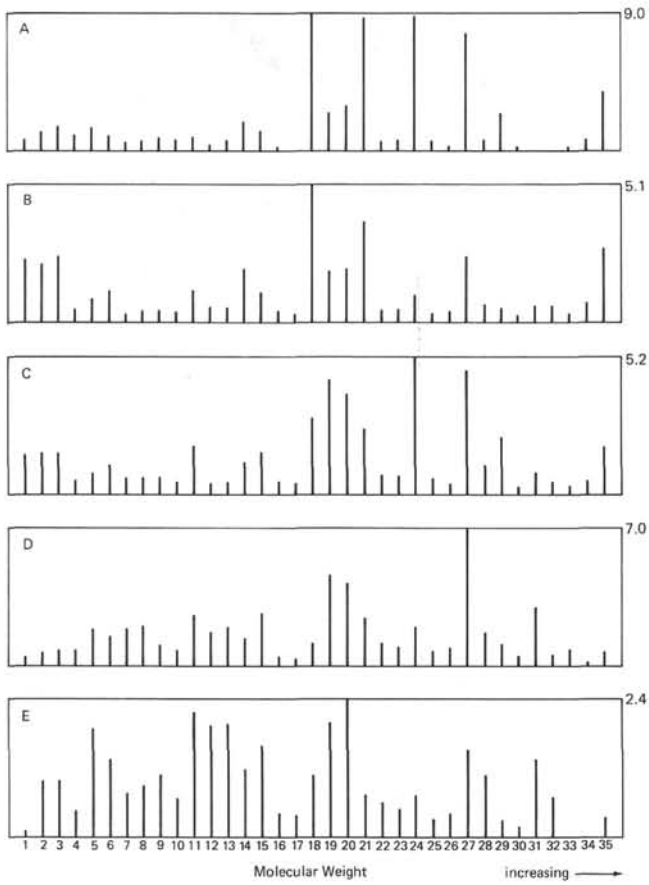

Figure 5. *Abundance (ng/g dry sediment) of aromatic components.* A. *Section 440A-7-6;* B. *Section 440B-3-5;* C. *Section 440B-8-4;* D. *Section 440B-68-2;* E. *Section 436-11-4. (Bar numbers refer to Table 8. Perylene concentrations [bar 21] must be multiplied by 13 to give true values; 3,3,7-trimethyl-1,2,3,4-tetrahydrochrysene [bar 27] concentration in A must be multiplied by 2.5 to give true value.)*

dimethylphenanthrenes X, $2CH_3$) remain constant and trimethylphenanthrenes (X, $3CH_3$) tend to increase. The amounts of fluoranthene (XI,H), pyrene (XII,H), chrysene (XIII,H), and their alkyl-homologues also tend to increase with increasing sample depth. A similar trend exists for most of the higher molecular weight PAH [e.g., benzo(g,h,i)perylene (XXII,H) and coronene (XXVII)], although perylene and methylperylene are exceptions to this trend.

Simonellite (XV) and retene (XIV) are the major aromatic diterpenoids in all samples. Simonellite decreases markedly with increasing depth, whereas retene remains relatively constant.

A series of monoaromatic steroids was identified in all Site 440 sections from MF (m/e 253) and comparison of GC retention times with Leg 50 data (Brassell et al., in press). The carbon number of the individual series members could not be determined because of the weakness (usually $<<1$ per cent of m/e 253) of their molecular ions. No aromatic steroids were detected in Section 436-11-4.

The trace concentrations of the major aromatic steroids in Sections 440B-3-5 and 440B-68-2 are roughly equal. Their distributions, as seen from MF, were similar in all the samples.

The presence of 18-nor- and 4-methyl aromatic steroids in trace quantities in Section 440B-68-2 was indicated by MF of their diagnostic ions, m/e 239 and m/e 267, respectively. These compounds were not detected in any of the other samples.

Assignments of the triterpenoid-derived aromatic compounds are tentative. The major triterpenoid-derived component was 3,3,7-trimethyl-1,2,3,4-tetrahydrochrysene (XXI) (Spyckerelle et al., 1977a), present in all the samples, with its greatest concentration in Section 440A-7-6. Two minor isomers (M^+ 274) of this compound, 5′-isopropyl-8-methyl-1,2-cyclopentenophenanthrene (XIX) and 3,4,7-trimethyl-1,2,3,4-tetrahydrochrysene (XX) (Spyckerelle, 1975), were also identified in all the samples. The concentration of both of these compounds increases with depth at Site 440.

The isomers 3,3,7,12a-tetramethyl-1,2,3,4,4a,11,12,12a-octahydrochrysene (XXV) and 3,4,7,12a-tetramethyl-1,2,3,4,4a,11,12,12a-octahydrochrysene (XXVI) (Spyckerelle et al., 1977b) were identified from their mass spectra (M^+ 292) and by MF. Both increase in concentration with depth at Site 440.

Two isomers (M^+ 324) were identified as; 3,4,10-trimethyl-1,2,3,4-tetrahydropicene (XXIX) and 3,3,10-trimethyl-1,2,3,4,-tetrahydropicene (XXX) (Streibl and Herout, 1969). The concentrations of both decrease with depth at Site 440.

Ethers

The distribution of sterol ethers and the concentrations of the major components of four of the samples are given in Table 9. These compounds were characterized by their individual mass spectra and by MF. Additional components were present in trace quantities in Section 440B-68-2. The sterol ethers of Section 440A-7-6 were similar to those of Section 440B-3-5 in both their distribution and concentration.

There are significant differences among the samples in the amounts and diversity of the sterol ethers. The complexity of sterol ether distribution appears to decrease with increasing depth at Site 440, although this may reflect the detection limit of analysis rather than a genuine trend.

The distribution of sterol ethers in Section 436-11-4 is somewhat similar to that of Section 440B-8-4, although their absolute amounts differ.

TABLE 8
Aromatic Hydrocarbon Concentrations (ng/g dry sediment)

Bar Number[a]	Compound(s)	Structure, R[b]	M^+	Section 440A-7-6	440B-3-5	440B-8-4	440B-68-2	436-11-4
1	Phenanthrene[c]	X, H	178	0.6	2.3	1.4	0.5	0.1
2	Methylphenanthrene[c]	X, CH_3	192	1.2	2.2	1.5	0.7	1.3
3	Methylphenanthrene[c]	X, CH_3	192	1.5	2.4	1.5	1.0	1.0
4	Fluoranthene[c]	XI, H	202	1.0	0.4	0.5	1.0	0.4
5	Pyrene[c]	XII, H	202	1.5	0.9	0.8	1.9	1.9
6	Dimethylphenanthrene[d, e]	X, $2CH_3$	206	1.0	1.2	1.1	1.6	1.4
N	Dimethyl-1,2,3,4-tetrahydrophenanthrene[d]		210	0.2	0.8	0.4	Tr	n.d.
7	Methylfluoranthene[d]	XI, CH_3	216	0.6	0.3	0.6	1.9	0.8
8	Methylpyrene[c]	XII, CH_3	216	0.6	0.4	0.6	2.1	0.9
9	Trimethylphenanthrene[d, f]	X, $3CH_3$	220	0.9	0.4	0.6	1.2	1.1
10	Trimethylphenanthrene[d, f]	X, $3CH_3$	220	0.7	0.4	0.5	1.0	0.7
11	Chrysene[c]	XIII, H	228	1.0	1.2	1.8	2.6	2.2
12	Dimethylfluoranthene[d, e]	XI, C_2H_5	230	0.4	0.6	0.4	1.8	2.0
13	Dimethylpyrene[d, e]	XII, C_2H_5	230	0.7	0.6	0.4	2.0	2.0
14	Retene(1-methyl-7-isopropylphenanthrene)[c]	XIV	234	2.0	2.0	1.2	1.5	1.2
15	Methylchrysene[d]	XIII, CH_3	242	1.2	1.1	1.6	2.7	1.6
16	Trimethylfluoranthene[d, f]	XI, C_3H_7	244	0.2	0.4	0.5	0.5	0.4
17	Trimethylpyrene[d, f]	XII, C_3H_7	244	n.d.	0.3	0.4	0.4	0.4
18	Simonellite(1,1-dimethyl-7-isopropyl-1,2,3,4-tetrahydrophenanthrene)[d]	XV	252	9.0	5.1	2.9	1.2	1.1
19	Benzofluoranthene[d]	XVI	252	2.4	1.9	4.3	4.6	2.0
20	Benzopyrene[d]	XVII	252	3.0	1.9	3.8	4.1	2.4
21	Perylene[c]	XVIII, H	252	113	48	32	31	9.2
22	Dimethylchrysene[d, e]	XIII, $2CH_3$	256	0.5	0.4	0.7	1.2	0.6
23	Dimethylchrysene[d, e]	XIII, $2CH_3$	256	0.5	0.5	0.7	1.0	0.5
24	Methylperylene[d]	XVIII, CH_3	266	8.8	1.0	5.2	2.0	0.7
25	8-methyl-5′-isopropyl-1,2-cyclopentano-phenanthrene[d]	XIX	274	0.5	0.3	0.6	0.8	0.3
26	3,4,7-trimethyl-1,2,3,4-tetrahydrochrysene[d]	XX	274	0.2	0.4	0.4	0.9	0.4
27	3,3,7-trimethyl-1,2,3,4-tetrahydrochrysene[d]	XXI	274	20	2.4	4.7	7.0	1.5
28	Benzo(ghi)perylene, anthanthrene, indenopyrene[d]	XXII, H; XXIII, H; XXIV, H	276	0.7	0.6	1.1	1.7	1.1
N[g]	Dimethylperylene[d, e]	XVIII, C_2H_5	280	0.4	0.2	0.2	1.2	0.3
29	Dimethylperylene[d, e]	XVIII, C_2H_5	280	2.4	0.5	2.2	1.1	0.3
30	Methylbenzo(ghi)perylene, methylanthanthrene	XXII, CH_3; XXIII, CH_3	290	0.2	0.2	0.3	0.5	0.2
N[g]	Methylindenopyrene[d]	XXIV, CH_3	290	0.1	n.d.	0.3	0.5	n.d.
31	3,3,7,12a-tetramethyl-1,2,3,4,4a,11,12,12a-octahydrochrysene[d]	XXV	292	n.d.	0.6	0.8	3.0	1.4
32	3,4,7,12a-tetramethyl-1,2,3,4,4a,11,12,12a-octahydrochrysene[d]	XXVI	292	n.d.	0.6	0.5	0.6	0.7
33	Coronene[d]	XXVII	300	0.2	0.3	0.3	0.8	n.d.
N[g]	3,3,7,10b,12a-pentamethyl-1,2,3,4,4a,4b,5,6,10b,11,12,12a-dodecahydrochrysene[d]	XXVIII	310	n.d.	0.2	0.1	1.2	0.3
34	3,4,10-trimethyl-1,2,3,4-tetrahydropicene[d]	XXIX	324	0.7	0.7	0.5	0.2	n.d.
35	3,3,10-trimethyl-1,2,3,4-tetrahydropicene[d]	XXX	324	3.9	2.8	1.8	0.7	0.4

Note: For explanation of Tr and n.d. see Note to Table 3.
[a] Bar number in Figure 5.
[b] See Appendix, this chapter.
[c] Assignments made from mass spectra and GC coinjection.
[d] Tentative assignments made by spectral interpretation, comparison with reference mass spectra, and GC retention data.
[e] Possibly ethyl.
[f] Possibly methylethyl or propyl.
[g] Not included in Figure 5.

Very Long Chain Ethers

Two novel compounds, tentatively identified as very long chain alkyl ethers, were detected as trace components of all samples. Identification of these compounds was based on the individual mass spectra obtained for neutral TLC fractions of Sections 440B-3-5 and 440B-8-4 and by comparison with data for identical compounds recognized in the lipid extract of the marine coccolithophore *Emiliania huxleyi* (Volkman, in press). These compounds were recognized from their GC retention times in those sections in which their presence could not be confirmed by MS.

The empirical formulae of these compounds, determined from their molecular ions, are $C_{38}H_{74}O$(M^+ 546) and $C_{39}H_{76}O$ (M^+ 560). The predominant M^+-31 (M^+-O-OCH_3) and M^+-45 (M^+-O-OC_2H_5) ions in their mass spectra and their TLC behavior (they coelute with sterol ethers) were used to assign them as methyl and ethyl ethers, respectively. The base peak in the mass spectrum of both compounds was m/e 96 (for spectra collected above m/e 50). In addition, they appear to be straight-chain compounds, as no ions indicative of favored cleavage at positions of branching are observed in their mass spectra, although authentic standards are necessary to confirm this hypothesis.

TABLE 9
Sterol Ether Concentrations (ng/g dry sediment)

Sterol Moiety[a]	Chain Length of Alkyl Moiety (R)[b]	M+	Section 440B-3-5	440B-8-4	440B-68-2	436-11-4
$C_{26:2}$	C_{10}	510	+	+	–	–
$C_{26:1}/C_{27:1}/C_{27:2}$	–	–	+	–	–	–
$C_{27:2}$	–	–	+	–	–	–
$C_{26:2}$	–	–	+	–	–	–
$C_{27:2}$	–	–	+	+	–	–
Δ^5-$C_{27:1}$	C_9	512	20	1.5	–	–
Δ^5-$C_{27:1}$	C_9	512	4	+	–	–
Δ^5-$C_{27:1}/C_{27:2}$	$C_{10}/C_{10:1}$	524	+++	+++	++	++
$C_{27:1}$	–	–	+	+	–	–
Δ^5-$C_{27:1}$	C_{10}	526	24	3	+++	2.5
Δ^5-$C_{28:1}$	C_9	526	++	++	–	–
$C_{27:2}/C_{28:2}$	C_{11}/C_{10}	538	+	1	–	2.5
$C_{27:1}$	C_{11}	540	+++	+	–	–
$C_{27:1}$	C_{10}	526	+	+	–	1
$C_{28:2}$	C_{10}	538	+	0.5	–	–
$C_{28:1}$	C_{10}	540	+	–	–	–
$C_{28:1}$	–	–	++	+	–	+
$C_{28:1}$	C_{10}	540	+	+	–	+
$C_{28:1}/C_{29:1}$	C_{11}/C_{10}	554	+	–	–	–
$C_{29:1}$	–	–	+	–	–	–
$C_{29:1}$	–	–	+	–	–	–
$C_{27:1}$	–	–	+	+	–	–
$C_{29:1}$	–	–	+	+	–	–
$C_{29:1}$	–	–	+	–	–	–

Note: +, ++, and +++ are qualitative estimates of relative concentrations.
[a]Δ-$C_{m:n}$ where m is carbon number, n is degree of unsaturation and Δ shows location of double bond.
[b]Structure XXXI, R – See Appendix, this chapter.

Although these ethers are present in only trace quantities in all the samples, it is possible to determine from a comparison of GC injection volumes that their concentration in Section 440B-68-2 is markedly lower than in the other samples.

Aliphatic Ketones

Normal Methyl Ketones

The concentrations of the individual methyl ketones, calculated from their GC response or by MF (m/e 58), are shown in Figure 6.

The odd-numbered members of the homologous series dominate in all samples, with C_{29} (nonacosan-2-one) as the major component, except in Section 440B-68-2, in which C_{25} dominates.

The proportion of C_{15} to C_{22} components is significantly lower in Section 436-11-4 than in the samples from Site 440. The overall distributions of Sections 440A-7-6, 440B-3-5, and 440B-8-4 are similar, whereas Section 440B-68-2 possesses a greater relative proportion of C_{20} to C_{25} components.

Branched/Cyclic

Monomethyl or other branched methyl ketones were not detected in any of the samples by MF of m/e 58. Minor quantities of ethyl ketones, either straight-chain or branched-chain, were observed in all samples by MF (m/e 72).

The concentration of 6,10,14-trimethylpentadecan-2-one in the five sections is given in Table 10. Identification of this component was based on its mass spectral characteristics and GC retention time. The quantity of 6,10,14-trimethylpentadecan-2-one decreases gradually with increasing depth of burial at Site 440 and is also significantly lower at Site 436 than the deepest Site 440 sample.

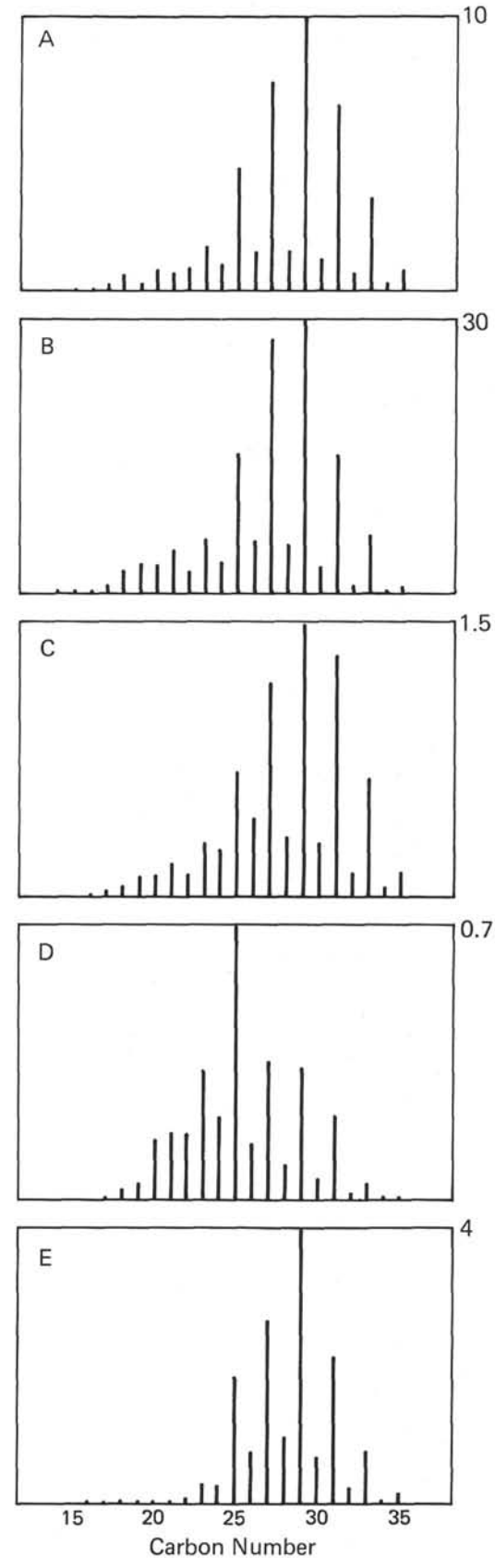

Figure 6. *Abundance (ng/g dry sediment) of* n*-methyl ketones.* A. *Section 440A-7-6;* B. *Section 440B-3-5;* C. *Section 440B-8-4;* D *Section 440B-68-2;* E. *Section 436-11-4.*

TABLE 10
C_{18} Isoprenoid Ketone Concentrations (ng/g dry sediment)

Section				
440A-7-6	440B-3-5	440B-8-4	440B-68-2	436-11-4
25	25	5	2	0.3

Various steroidal ketones were present in all the Site 440 sections, but these components could not be confirmed as constituents of Section 436-11-4. These compounds were recognized from MF of diagnostic ions for stenones (m/e 229), stanones (m/e 231), 4-methylstenones (m/e 285), and 4-methylstanones (m/e 245), but none of the compounds was present in sufficient quantity (>1 ng/g dry sediment) to enable an unambiguous assignment from its mass spectrum. In particular, the dominance of the long-chain ketones in the steroidal ketone fraction of Section 440B-7-6 precluded even the comparison of key mass fragmentograms with those of the other Site 440 sections. The information that could be deduced from the various mass fragmentograms is summarized as follows:

1) m/e 229; stenones. A single major component is present in Sections 440B-3-5 and 440B-8-4. On the evidence of mass fragmentogram multiplication factors, this compound is the most abundant steroidal ketone in these samples.

2) m/e 231; stanones. The distributions of these compounds in Sections 440B-3-5, 440B-8-4, and 440B-68-2 are markedly different. The complexity of these mass fragmentograms decreases with increasing sample depth.

3) m/e 285; mainly 4-methylstenones. Two major components are observed in Sections 440B-3-5 and 440B-68-2. The earlier-eluting compound is dominant in Section 440B-3-5, whereas Section 440B-68-2 contains the two components in equal abundance.

4) m/e 245; 4-methylstanones. Sections 440B-3-5, 440B-8-4, and 440B-68-2 are similar in terms both of distribution and relative proportions of these compounds.

The major hopanoid ketones, recognized from their full mass spectra and GC retention times, are quantitated in Table 11. A considerable number of minor compounds was also observed in the m/e 191 mass fragmentograms of the Site 440 Sections, showing that the range of hopanoid ketones is more diverse than Table 11 suggests. It seems probable that several of these additional components are stereoisomers of the compounds recognized.

Sections 440A-7-6 and 440B-3-5 are generally similar in their hopanoid ketone distributions. Trisnorhop-21-one is the most abundant component in all the sections. Section 440B-68-2 is the only sample with a detectable quantity of homohop-29-one.

No hopenones were detected in any of the sections.

In every section various non-hopanoid triterpenoid ketones were tentatively identified from their mass spectra (by comparison with literature spectra) (Wardroper, personal communication), GC retention times, and by MF of diagnostic ions. The compounds recognized, which are all 3-ones, are quantified in Table 12, although only traces (<1 ng/g) were detected in Sections 440B-8-4 and 436-11-4. In addition to the components tabulated, a number of other unknown compounds were also present whose structures could not be assigned from their mass spectra.

Friedelan-3-one is only present in significant amounts in Section 440B-3-5, whereas olean-12(12)-en-3-one and urs-12(12)-en-3-one were detected in all Site 440 sections. No trend with depth in the distribution of non-hopanoid ketones is discernible at Site 440.

Very Long Chain Unsaturated Ketones

A number of very long straight-chain C_{37}, C_{38}, and C_{39} unsaturated ketones were present in all five samples. These novel compounds were identified by GC coinjection and mass spectral comparison with identical compounds isolated from the unicellular coccolithophore *Emiliania huxleyi* (Volkman, in press). The presence of double bonds and the absence of ring structures in the algal ketones were confirmed by hydrogenation and the existence of the ketone group itself verified by formation of the methoxime derivatives. A typical gas chromatogram of the ketones after TLC fractionation is shown in Figure 7, and the concentrations of the eight major components in the five sections, calculated from GC responses, are given in Table 13. Series of methyl and ethyl ketones were detected, and for Sections 436-11-4 and 440B-68-2, these were separated by the second TLC fractionation of neutral components. Methyl ketones gave mass spectra with their base peak at m/e 43 ($COCH_3$; or m/e 96 for spectra collected from m/e 50) and significant ions at M^{+}-18 (M^{+}-H_2O), M^{+}-43 (M^{+}-$COCH_3$), and M^{+}-58 (McLafferty rearrangement), typical of this compound class. Ethyl ketones gave a base peak of m/e 57 and key ions at M^{+}-18 (M^{+}-H_2O), M^{+}-29 (M^{+}-C_2H_5), and M^{+}-72 (McLafferty rearrangement). Molecular ions for all compounds were weak but discernible. In each spectrum, an exponential-type decrease in ion intensity with increasing m/e value was consistent with the presence of a long, unsaturated aklyl chain. No favored mass spectral fragmentations suggestive of cleavage at positions of branching were present, although in the absence of authentic standards, the existence of methyl branches cannot be unequivocably excluded. No evidence for propyl or longer alkyl chain ketones was obtained, although in several samples, notably Section 440B-3-5, GC evidence suggested the presence of C_{40} and longer chain ketones (Figure 7). The low quantities of these compounds prevented their characterization.

All of the major components contained either two or three double bonds. No corresponding monounsaturated and saturated ketones were detected. The double bond positions have not been determined, although the presence of single symmetrical peaks for each component in capillary GC analysis suggests that each ketone is a single compound, not a mixture of double bond positional isomers.

TABLE 11
Hopanoid Ketone Concentrations (ng/g dry sediment)

	Structure R	Section 440A-7-6	440B-3-5	440B-8-4	440B-68-2	436-11-4
Trisnorhop-21-one	XXXII	Tr	1	Tr	Tr	n.d.
Trisnorhop-21-one	XXXII	10	10	1	1.5	Tr
Norhop-22-one	VI, R:$C(CH_3)O$	1.5	4	Tr	Tr	n.d.
Homohop-29-one	VI, R:$CH(CH_3)COCH_3$	n.d.[a]	Tr	n.d.[a]	1	n.d.
Trishomohop-32-one	VI, R:$CH(CH_3)(CH_2)_2COCH_3$	2	n.d.[a]	Tr	n.d.	n.d.

Note: For explanation of Tr and n.d. see Note to Table 3.
[a]Compound possibly present but experimental conditions precluded detection.
[b]Stereochemistry not assigned – see Appendix, this chapter.

TABLE 12
Triterpenoid Ketone Concentrations (ng/g dry sediment)

	Structure[a]	Section 440A-7-6	440B-3-5	440B-8-4	440B-68-2	436-11-4
Taraxer-14-en-3-one	XXXIII	n.d.	1	n.d.	n.d.	n.d.
Olean-12(12)-en-3-one	XXXIV	3	5	Tr	2	Tr
Urs-12(12)-en-3-one	XXXV	2	4	Tr	2	n.d.
Glut-5-en-3-one	XXXVI	n.d.	n.d.	n.d.	Tr	n.d.
Friedelan-3-one	XXXVII	Tr	5	Tr	n.d.	n.d.

Note: For explanation of Tr and n.d., see Note to Table 3.
[a]See Appendix, this chapter.

The concentration of very long chain ketones is highest in Sections 440A-7-6 and 440B-3-5. In comparison with these samples, Sections 440B-8-4 and 436-11-4 contain markedly lower concentrations, whereas the value for Section 440B-68-2 is an order of magnitude lower. The ratios of the methyl to ethyl ketones of all the Site 440 sections are similar, whereas the value for Section 436-11-4 is markedly higher. The ratios of the diunsaturated to triunsaturated ketones of Sections 440A-7-6, 440B-3-5 and 440B-8-4 are similar, whereas the value for Section 436-11-4 is slightly greater and that of Section 440B-68-2 higher still.

Very long mid-chain ketones (e.g., C_{31} - C_{43}) such as those observed in Walvis Bay diatomaceous ooze (Boon and de Leeuw, 1979) were not detected.

Aliphatic Alcohols

Normal

The concentrations of *n*-alkan-1-ols, calculated by GC or MF (m/e 75) of their trimethylsilyl ethers, are shown in Figure 8.

In all samples, the even-numbered members of the homologous series are the dominant components, maximizing at C_{24} (C_{22} for Section 440B-3-5). The proportions of C_{11} to C_{22} alcohols (especially C_{16} and C_{22}) in Sections 440A-7-6, 440B-3-5, and 440B-8-4 are markedly higher than in Sections 440B-68-2 and 436-11-4.

In all samples a series of monoenoic alcohols was detected (Figure 9). Each component was characterized from the mass spectrum of its TMS ether (base peak M^+ -15). The $C_{24:1}$ alcohol is the major monoenoic alcohol in every sample, and the even-numbered alkenols predominate over the odd-numbered members. The amounts of alkenols in Section 436-11-4 are markedly lower than those in sections of Site 440.

Branched/Cyclic

A series of monomethyl branched alcohols, characterized (as their TMS ethers) from their mass spectra and GC retention times, was detected in all Site 440 samples (Figure 10). Section 436-11-4 contained C_{22} to C_{28} components in detectable, though trace (<1 ng/g), quantities.

The even-numbered branched alcohols appear to be present as single isomers (iso-alcohols), whereas the odd-numbered members of the series occur as at least two isomers recognized as iso- and anteiso-isomers for the C_{15} component. In all samples, the C_{24} iso-alcohol is the major component, and in general the even-numbered iso-alcohols dominate the odd-numbered isomers with the exception of C_{15}. The proportion of iso- and anteiso-pentadecanol in Sections 440A-7-6 and 440B-3-5 is markedly higher than in Sections 440B-8-4 and 440B-68-2.

The concentration of phytol, characterized from its mass spectrum and GC retention time, in Sections 440A-7-6, 440B-3-5, and 440B-8-4 is given in Table 14. No phytol was detected in Sections 440B-68-2 or 436-11-4, and neither dihydrophytol nor lower isoprenoid alcohols were detected in any of the sections.

The concentrations of selected sterols (XXXVIII) and 5α-stanols (XXXIX) (in ng/g dry sediment wt.), calculated from GC or by MF of m/e 215 for Section 436-11-4, are shown in Figure 11. In addition, a considerable number of minor sterols have been characterized in Section 440B-3-5, in which TLC separation gave a discrete sterol/5α-stanol fraction free of *n*-alcohols. The minor sterols recognized from their mass spectra included 24-ethylidenecholest-5-en-3β-ol; 24-ethylidene-5α-cholestan-3β-ol; 24-propylidenecholest-5-en-3β-ol, 24-propylidene-5α-cholestan-3β-ol; 5α-gorgostanol; and C_{21}, C_{22}, C_{23}, and C_{24} 5α-stanols, with C_2 to C_5 side chains.

The sterol/5α-stanol composition of Sections 440A-7-6 and 440B-3-5 is similar, whereas the proportion of C_{27} sterols/5α-stanol is higher in Section 440B-8-4 and

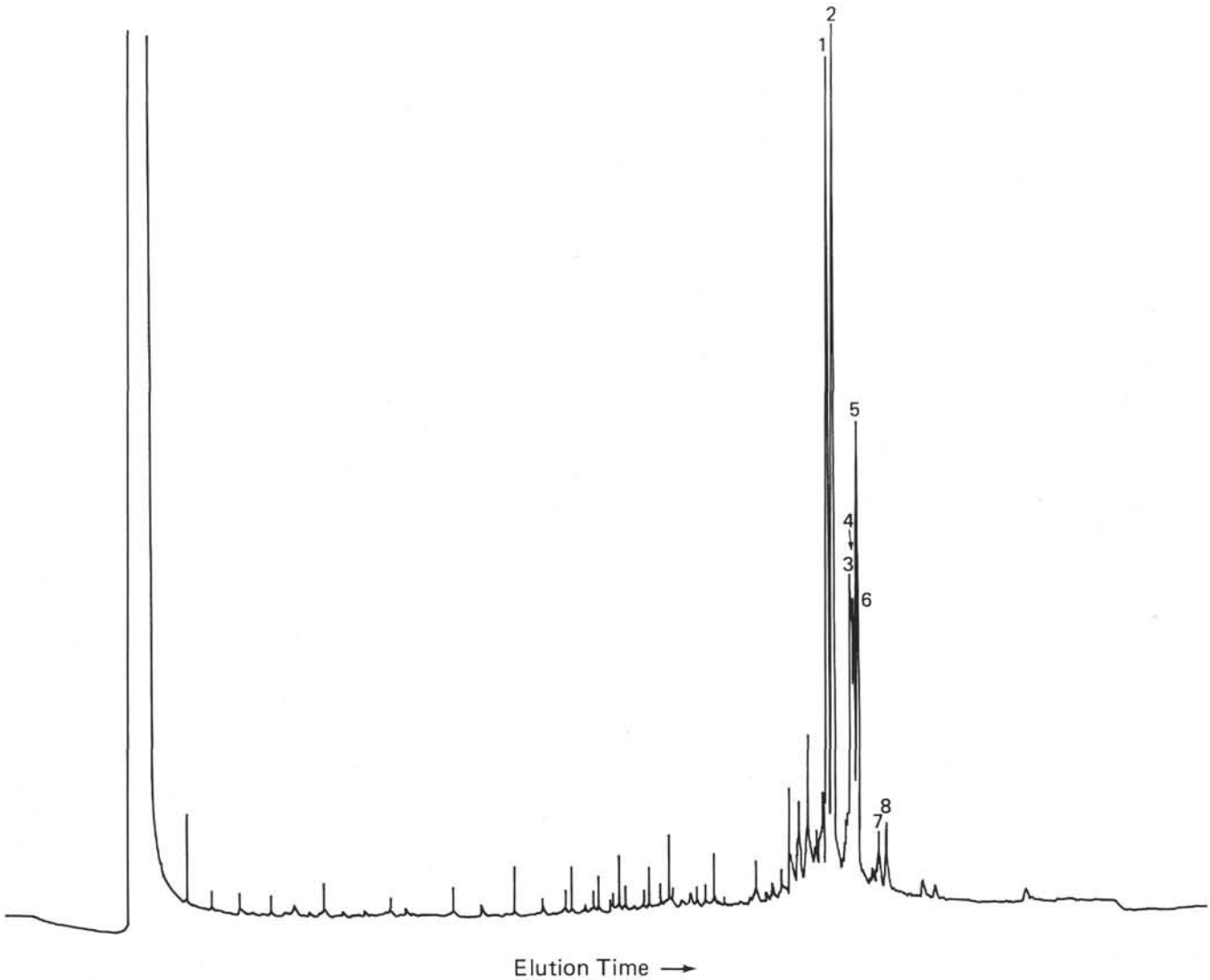

Figure 7. *Typical gas chromatogram of very long chain unsaturated ketones (Section 440B-3-5). As follows: 1. $C_{37:3}$ methyl ketone; 2. $C_{37:2}$ methyl ketone; 3. $C_{38:3}$ ethyl ketone; 4. $C_{38:3}$ methyl ketone; 5. $C_{38:2}$ ethyl ketone; 6. $C_{38:2}$ methyl ketone; 7. $C_{39:3}$ ethyl ketone; 8. $C_{39:2}$ ethyl ketone. (For GC conditions, see Experimental Procedures.)*

TABLE 13
Concentrations (ng/g dry sediment) of Very Long Chain Unsaturated Ketones

	Methyl Ketones				Ethyl Ketones								
GC Peak[e] Section	37:3 1	37:2 2	38:3 4	38:2 6	38:3 3	38:2 5	39:3 7	39:2 8	Total Ketones	Me/Et[a]	Di/Tri[b]	Di/Total[c]	Tri/Total[d]
440B-7-6	180	220	56	71	54	110	9.0	15	715	2.8	1.4	0.58	0.42
440B-3-5	180	190	68	71	69	104	17	20	719	2.4	1.2	0.54	0.46
440B-8-4	35	37	11	11	10	17	2.4	2.7	126	2.9	1.2	0.54	0.46
440B-68-2	4.4	18	1.2	3.7	1.7	7.6	0.3	0.9	38	2.6	4.0	0.80	0.20
436-11-4	59	111	14	27	8.5	19	1.2	3.0	243	7.0	1.9		

[a] Ratio of total methyl:total ethyl.
[b] Ratio of total diunsaturates:total triunsaturates.
[c] Ratio of total diunsaturates:total ketones.
[d] Ratio of total triunsaturates:total ketones.
[e] See Figure 7.

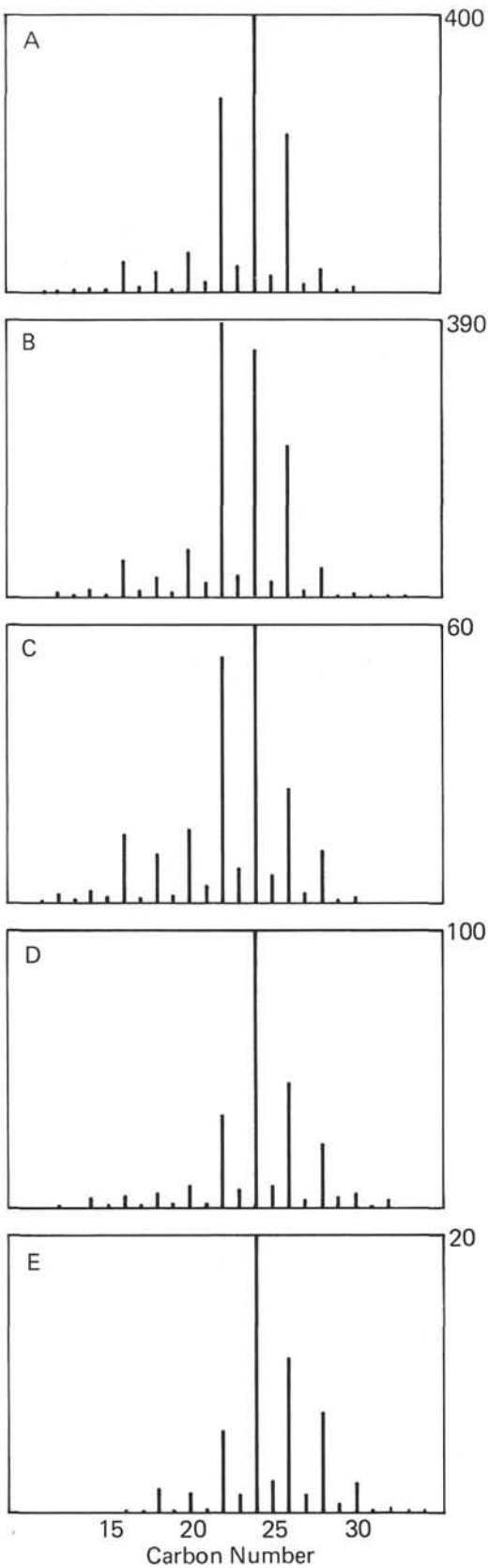

Figure 8. *Abundance (ng/g dry sediment) of* n-*alcohols determined as TMS derivatives.* A. *Section 440A-7-6;* B. *Section 440B-3-5;* C. *Section 440B-8-4;* D. *Section 440B-68-2;* E. *Section 436-11-4.*

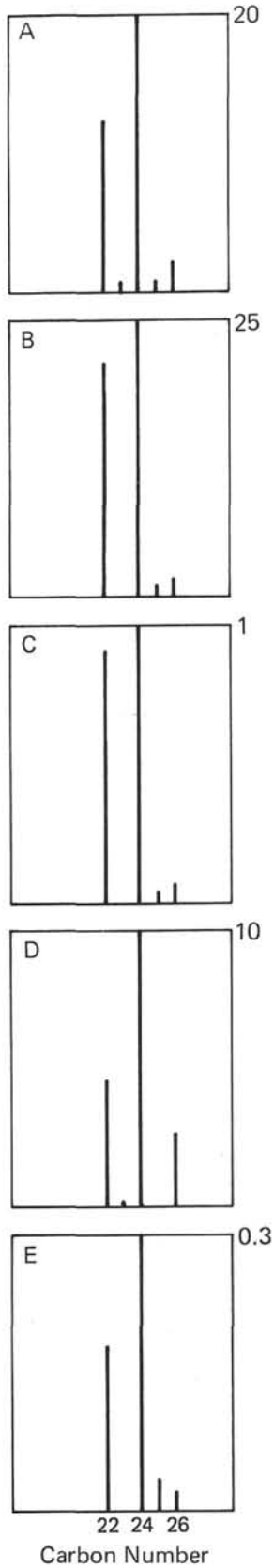

Figure 9. *Abundance (ng/g dry sediment) of monoenoic* n-*alcohols, determined as TMS derivatives.* A. *Section 440A-7-6;* B. *Section 440B-3-5;* C. *Section 440B-8-4;* D. *Section 440B-68-2;* E. *Section 436-11-4.*

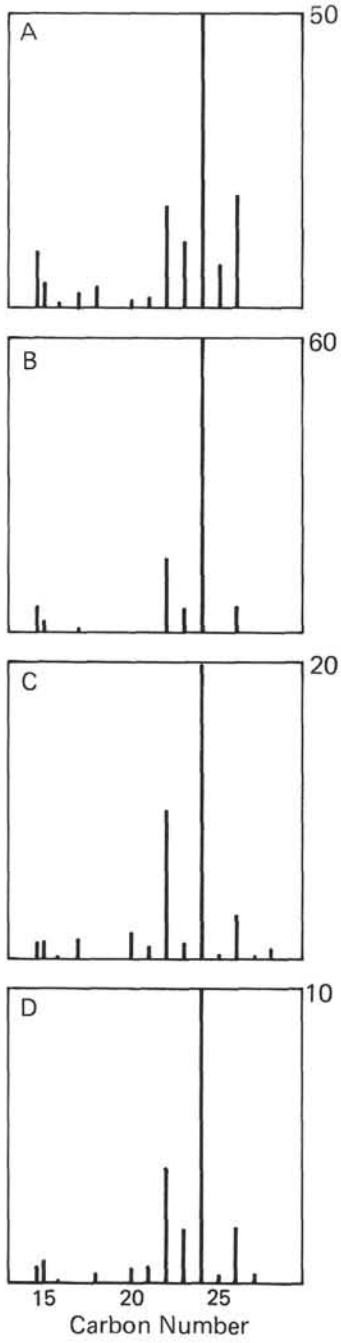

Figure 10. *Abundance (ng/g dry sediment) of monomethyl branched alcohols, determined as TMS derivatives.* A. *Section 440A-7-6;* B. *Section 440B-3-5;* C. *Section 440B-8-4;* D. *Section 440B-68-2.*

TABLE 14
Phytol Concentrations

	Section		
	440A-7-6	440B-3-5	440B-8-4
Phytol concentration (ng/g dry sediment)	140	139	13

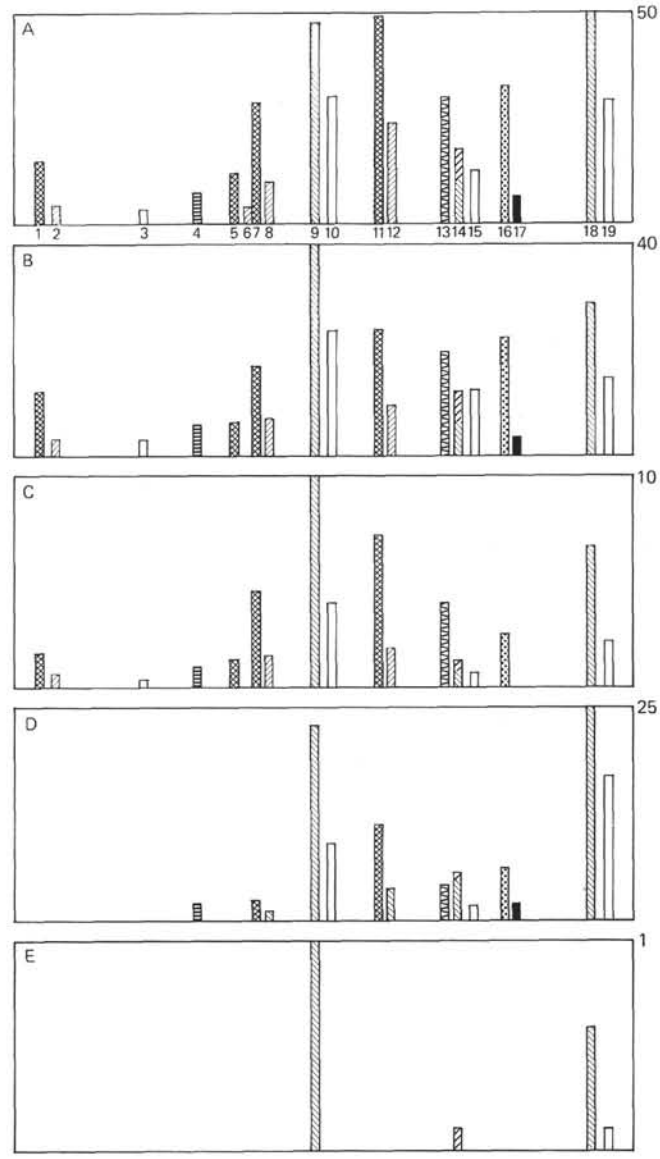

Figure 11. *Abundance (ng/g sediment) of selected sterols and 5α-stanols, determined as TMS derivatives.* A. *Section 440B-7-6;* B. *Section 440B-3-5;* C. *Section 440B-8-4;* D. *Section 440B-68-2;* E. *Section 436-11-4. Bar numbers correspond as follows: 1. 22-*trans*-24-norcholesta-5,22-dien-3β-ol (XL,*$\Delta^{5,22}$*); 2. 22-*trans*-24-nor-5α-cholest-22-en-3β-ol (XL,*Δ^{22}*,5α); 3. 5α-24-norcholestan-3β-ol (XL,5α); 4. 5β-cholestan-3β-0l (XXXIX, R:H,R':H,5β); 5. C_{27}-5,22-dien-3β-ol (XXXVIII, R:H,R':H,*$\Delta^{5,22}$*); 6. 5α-C_{27}-22-en-3β-ol (XXXIX, R:H,R',*Δ^{22}*,5α); 7. 22-*trans*-cholesta-5,22-dien-3β-ol (XXXVIII, R:H,R':H,*$\Delta^{5,22}$*); 8. 22-*trans*-5α-cholest-22-en-3β-ol (XXXIX, R:H,R':H,*Δ^{22}*,5α); 9. cholest-5-en-3β-ol (XXXVIII, R:H,R':H,*Δ^{5}*); 10. 5α-cholestan-3β-ol (XXXIX, R:H,R':H,5α); 11. 24-methylcholestan-5,22,dien-3β-ol (XXXVIII, R:CH_3,R':H,*$\Delta^{5,22}$*); 12. 24-methyl-5α-cholest-22-en-3β-ol (XXXIX, R:CH_3,R':H,*Δ^{22}*,5α); 13. 24-methylenecholest-5-en-3β-ol (XXXVIII, R: = CH_2,R':H,*Δ^{5}*); 14. 24-methylene-5α-cholestan-3β-ol (XXXIX, R: = CH_2,R':H,5α) and 24-methylcholest-5-en-3β-ol (XXXVIII, R:CH_3,R':H,*Δ^{5}*); 15. 24-methyl-5α-cholestan-3β-ol (XXXIX, R:CH_3,R':H,5α); 16. 23,24-dimethylcholesta-5,22-dien-3β-ol (XXXVIII, R:CH_3, R':CH_3,*$\Delta^{5,22}$*); 17. 23,24-dimethyl-5α-cholest-22-en-3β-ol (XXXIX, R:CH_3R':CH_3,*Δ^{22}*,5α); 18. 24-ethylcholest-5-en-3β-ol (XXXVIII, R:C_2H_5,R':H,*Δ^{5}*); 19. 24-ethyl-5α-cholestan-3β-ol (XXXIX, R:C_2H_5,R':H,5α) and 24-ethylidenecholest-5-en-3β-ol (XXXVIII, R: = $CHCH_3$,R':H,*Δ^{5}*).*

Section 440B-68-2 possesses noticeably lower quantities of the C_{28} components. These differences can be seen in Figure 11. The sterol/5α-stanol content of Section 436-11-4 is extremely low; because identification of even the major sterols is difficult, the reliability of the tentative assignments in Figure 11 is questionable.

5β-stanols were identified in all the Site 440 samples. In each instance the dominant compound was 5β-cholestan-3β-ol (Figure 11), whereas 24-methyl-5β-cholestan-3β-ol and 24-ethyl-5β-cholestan-3β-ol, were present in trace amounts. No 5β-stanols were detected in Section 436-11-4.

The proportion of 5β-stanols decreases with increasing sample depth at Site 440, although the distributions of C_{27}, C_{28}, and C_{29} compounds, as seen in MF of m/e 215, were similar.

4-methyl stenols and 4-methyl stanols were identified by MF and full mass spectra in the four samples from Site 440, whereas Section 436-11-4 did not contain these components in detectable quantities.

Three extended hopanoid alcohols were detected, all with the hydroxy group in their side chain. They were characterized by MF (m/e 191, 203, and 217) and from their full mass spectra. The distribution of these hopanoid alcohols in the Site 440 sections is given in Table 15. No hopanoid alcohols were detected in Section 436-11-4.

The distribution of the three components in the four sections is similar, though their quantities in Section 440B-8-4 are considerably lower than those of the other Site 440 sections.

Fatty Acids (free and bound)

Fatty acids were characterized from their GC retention times and MF of diagnostic ions (e.g., m/e 74 and 87 for *n*-fatty acids). The total concentrations of each fatty acid fraction are given in Table 16 and show considerable fluctuations in the Site 440 values. The distributions of fatty acids in all samples are generally similar; an example is shown in Figure 12.

Free Normal Fatty Acids

The free *n*-fatty acid distribution is bimodal, peaking at *n*-C_{16} and *n*-C_{26}. The proportions of low to high carbon number acids (i.e., C_{10}-C_{20} to C_{21}-C_{30}) show slight variation. For instance, Section 436-11-4 contains greater relative amounts of high carbon number acids than most of the other Site 440 sections. The high carbon number acids predominate in all samples. All sections have a pronounced C.P.I.

TABLE 15
Hopanoid Alcohol Concentration (ng/g dry sediment)

		Section			
	Structure[b]	440A-7-6	440B-3-5	440B-8-4	440B-68-2
17βH,21βH-homohopan-31-ol	VI, R:CH(CH_3)(CH_2)$_2$OH	3	1	Tr	1
17βH,21βH-bishomohopan-32-ol	VI, R:CH(CH_3)(CH_2)$_3$OH	9	5	Tr	3
C_{33} hopanol[a]		1.5	Tr	n.d.	Tr

Note: For explanation of Tr and n.d. see Note to Table 3.
[a]17αH,21βH-trishomohopan-33-ol or 17βH,21βH-trishomohopan-33-ol.
[b]See Appendix, this chapter.

TABLE 16
Concentrations of Acidic Components (ng/g dry sediment)

	Monoacids						Unsaturated Acids (16:1 + 18:1)	
	Free		Bound		Diacids			
Section	*n*-C_{10}-*n*-C_{20}	*n*-C_{21}-*n*-C_{32}	*n*-C_{10}-*n*-C_{20}	*n*-C_{21}-*n*-C_{32}	Free	Bound	Free	Bound
440A-7-6	6.2	6.7	73	8.6	n.d.	40	Tr	2
440B-3-5	65	111	15	3	20	7	3	8
440B-8-4	5.2	6.1	37.5	14.4	10	11	n.d.	18
440B-68-2	45	96	6.2	3.1	85	8	2	Tr
436-11-4	30	56	3.6	1.1	3	2	20	1

Hydroxyacids (All Bound)

	ω-OH	Straight-Chain β-OH	Branched β-OH	Cutin Acids (C_{16} di-OH; C_{18} tri-OH, etc.)
440A-7-6	2.5	6.7	8.6	3.0
440B-3-5	2.0	1.4	1.4	0.2
440B-8-4	5.5	1.3	1.2	0.4
440B-68-2	Tr	n.d.	n.d.	n.d.
436-11-4	0.6	0.1	0.1	n.d.

Note: For explanation of Tr and n.d. see Note to Table 3.

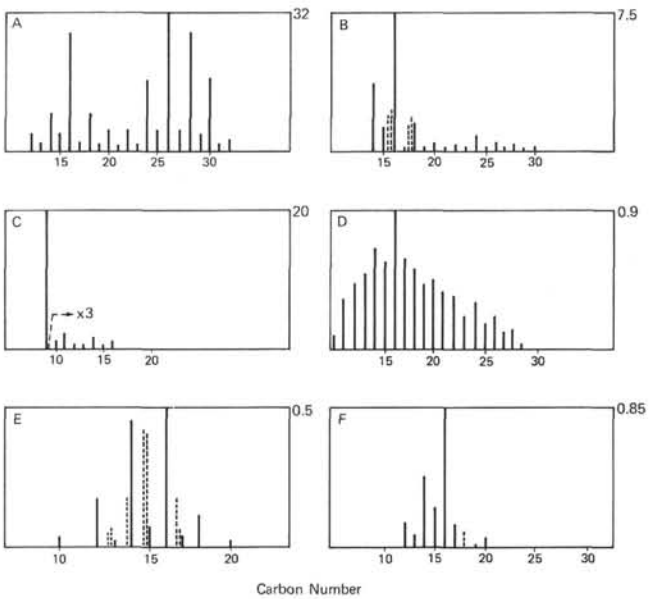

Figure 12. *Abundance (ng/g dry sediment) of carboxylic acids (determined as methyl esters) in Section 440B-3-5. A. free* n*-fatty acids, ---- signifies unsaturated components; B. bound* n*-fatty acids, ---- signifies unsaturated components; C. free α,ω dicarboxylic acids; D. bound α,ω dicarboxylic acids; E. bound β-hydroxy acids, ---- signifies iso- and anteiso- components; F. bound ω-hydroxy acids, ---- signifies unsaturated component.*

Bound Normal Fatty Acids

The bound *n*-fatty acids show different bimodal distributions from the free *n*-fatty acids in that their higher carbon number maxima are much less developed than their lower carbon number maxima. High carbon number *n*-fatty acids are therefore present in lower abundance, relative to low carbon number *n*-fatty acids, in

the bound fractions than in the free fractions. The bound *n*-fatty acids, like the free *n*-fatty acids, have pronounced C.P.I. values. There appears to be an inverse correlation between the concentrations of free and bound *n*-fatty acids.

Unsaturated Fatty Acids

$C_{16:1}$ and $C_{18:1}$ monounsaturated fatty acids were detected in both the free and the bound fractions of all samples except Section 440B-8-4. In general, the amounts present varied with the saturated fatty acid content. The only polyunsaturated acid detected was trace amounts of $C_{18:2}$ in Section 440B-3-5. No branched unsaturated acids were detected in any of the samples.

α,ω-Dicarboxylic Acids

α,ω-dicarboxylic acids are present in the acid fractions of all samples except 440A-7-6. No unsaturated diacids were detected.

Free Diacids

Free *n*-diacids were recognized in all samples except Section 440A-7-6 and are particularly abundant in Section 440B-68-2. In each case the dominant component is the *n*-C_9 diacid with smaller amounts of higher homologues (*n*-C_{10} - *n*-C_{16}, showing a definite C.P.I.) also present. Branched C_9 and C_{11} diacids were tentatively identified in Section 440B-68-2 from their mass spectral similarities to the *n*-C_9 and *n*-C_{11} diacids, respectively, and also from their GC retention times as they eluted just prior to their normal isomers.

The major component of a small (0.5 g) DSDP sample from Leg 63 (467-110-3) was identified as dibutyl nonadioate and probably arises from either the plastic sampling bags or the core liner. The free diacid distribution may therefore be rationalized mainly in terms of saponified plasticizer rather than natural oxidative breakdown of acids with Δ^9 unsaturation.

Bound Diacids

The bound α,ω-dicarboxylic acids show a different and markedly more complex distribution compared with the free diacids. The *n*-C_{16} diacid is the major component, whereas the *n*-C_9 diacid is only a minor component when present. Significant amounts of higher carbon number homologues (*n*-C_{20} - *n*-C_{29}) also occur in the bound diacid fractions. Three of the samples (Sections 440A-7-6, 440B-3-5, and 436-11-4) show unimodal distributions, maximizing at *n*-C_{16}. The other two sections possess bimodal distributions with Section 440B-8-4 maximizing at *n*-C_{16} and *n*-C_{21}, whereas Section 440B-68-2 peaks at *n*-C_{13} and *n*-C_{16}. The C.P.I. values for the bound diacid fractions are almost unity. No unsaturated or branched diacids were detected among the bound diacids.

Branched/Cyclic Acids

Iso- and anteiso-C_{15} acids are minor components of all the samples. Isoprenoid acids derived from phytol are not present above trace quantities in any of the sections. However, small amounts of pristanic and phytanic acids were recognized in the bound acid fraction of Section 440B-68-2. No unsaturated isoprenoid acids (e.g., phytenic acid) were detected in either free or bound fractions. No diterpenoid acids were found in the free acid fractions, though MF (m/e 239) suggested that trace amounts were present in the bound fraction of Section 440A-7-6. Steroidal acids (e.g., 5α-cholanic acid) were not detected in any of the samples. Small amounts of 17βH,21αH-bishomohopanoic acid were recognized in all the sections. No hopenoic acids were detected.

Hydroxy Fatty Acids

Hydroxy fatty acids only occur in the bound acid fractions. They can be conveniently grouped into four major categories: α-OH, β-OH, ω-OH, and cutin acids.

α-OH Acids

α-hydroxy acids are minor components of the samples, though Section 440A-7-6 contains *n*-C_9α-OH acid as a major hydroxy acid. In Section 440B-68-2 a small amount of *n*-C_{16}α-OH acid and traces of higher homologues were detected. No unsaturated α-OH acids were recognized in any of the samples.

β-OH Acids

β-hydroxy acids were recognized from their characteristic mass spectral fragmentation (m/e 175). The β-OH acid concentrations in Site 440 samples show a decrease with increasing depth, and none were detected in Section 440B-68-2 (Table 16). The samples all show a similar unimodal β-OH acid distribution, maximizing at either *n*-C_{16} (Sections 440A-7-6 and 436-11-4) or *n*-C_{14} (Sections 440B-3-5 and 440B-8-4). In the C_{10} to C_{18} range the β-OH acids show a marked even over odd preference, and traces of higher homologues ($>C_{22}$) were recognized in Section 440B-8-4. A significant feature of the β-OH acid distributions is the presence of relatively large amounts of iso- and anteiso- C_{13}, C_{15}, and C_{17} components with C_{15} dominant. No unsaturated β-OH acids were detected in any of the sections.

ω-OH Acids

ω-hydroxy acids were characterized by MF (m/e 146) and mass spectral comparisons with authentic standards. These compounds are present in all sections, generally possessing unimodal distributions maximizing at *n*-C_{16}. Sections 440A-7-6 and 440B-8-4 also show minor secondary modes maximizing at *n*-C_{20} and *n*-C_{22}, respectively. The ω-OH acid distributions resemble those of the bound dicarboxylic acids, except that they show a more pronounced C.P.I. An unsaturated $C_{18:1}$ω-OH acid and an *n*-C_{16}(ω-1)-OH acid were detected in all the samples except Section 440B-68-2.

Cutin Acids

Small amounts of cutin acids were detected in Sections 440A-7-6, 440B-3-5, and 440B-8-4, with *n*-C_{16} dihydroxy acids as the principal components. The concentration of cutin acids is greatest in Section 440A-7-6. Three *n*-C_{16} dihydroxy acid isomers 7,16, 9,16, and

10,16 were characterized in the samples, with the 9,16 isomer dominant (Figure 12). Several isomeric mid-chain hydroxy $C_{16}\alpha,\omega$-dicarboxylic acids and a single C_{18} trihydroxy acid were also found (Table 16).

Humic Acids

Humic acids (HAs) from Sections 440A-7-6, 440B-68-2, and 436-11-4 were examined. Yields and elemental analyses are given in Table 17. The two high ash contents reflect how their extraction procedure is susceptible to contamination by clay minerals.

HA-carbon constitutes only a small amount of the total organic carbon (<6 per cent) in each sample (nearest available section values of total organic carbon taken). The content is least in the oldest sediment (Section 440B -68-2).

Oxygen contents in the elemental analyses were calculated by difference. Some errors are likely in those data for the high ash content HAs (>10 per cent), where H and O can be contributed from clay minerals at the temperature of analysis. The conditions of alkaline reflux in the extraction of bound components could also have caused partial degradation and/or oxidative polymerization of the HA macromolecules. Since phenolic components were not detected in the bound acid fraction, it is unlikely that extensive degradation occurred.

The simplest formulae and elementary cells of each HA were computed from their elementary compositions. Assuming one sulphur atom per elementary cell, the formulae and molecular weights are as follows:

HA-440A-7-6	$C_{39}H_{48}O_{14}N_3S$	814
HA-440B-68-2	$C_{48}H_{80}O_{32}N_3S$	1242
HA-436-11-4	$C_{34}H_{49}O_{16}N_3S$	787

The visible spectra from 350 to 700 nm are typical of HAs, being largely structureless and showing a monotonic increase in absorbance with decrease in wavelength. In each case, a 20-nm-wide shoulder is present at 410 nm (Figure 13), together with possible weak bands in the region 600 to 660 nm. Values for the ratio of absorbance at 400 nm to that at 600 nm (E400/600) were computed for each HA (Table 17).

The IR spectra of HAs from Sections 440B-68-2 and 436-11-4 are complicated by strong absorptions due to

TABLE 17
Humic Acid Data

		Section 440A-7-6	440B-68-2	436-11-4
Yield (mg/g)		0.98	0.37	0.53
Ash Content (%)		1.3	21.0	13.3
Elemental Composition (%)	C	56.4	46.2	51.0
	H	5.9	6.5	6.1
	N	5.7	3.5	6.0
	S	3.9	2.6	4.0
	O	28.1	41.2	32.9
$E_{400/600}$		5.86	3.35	3.29

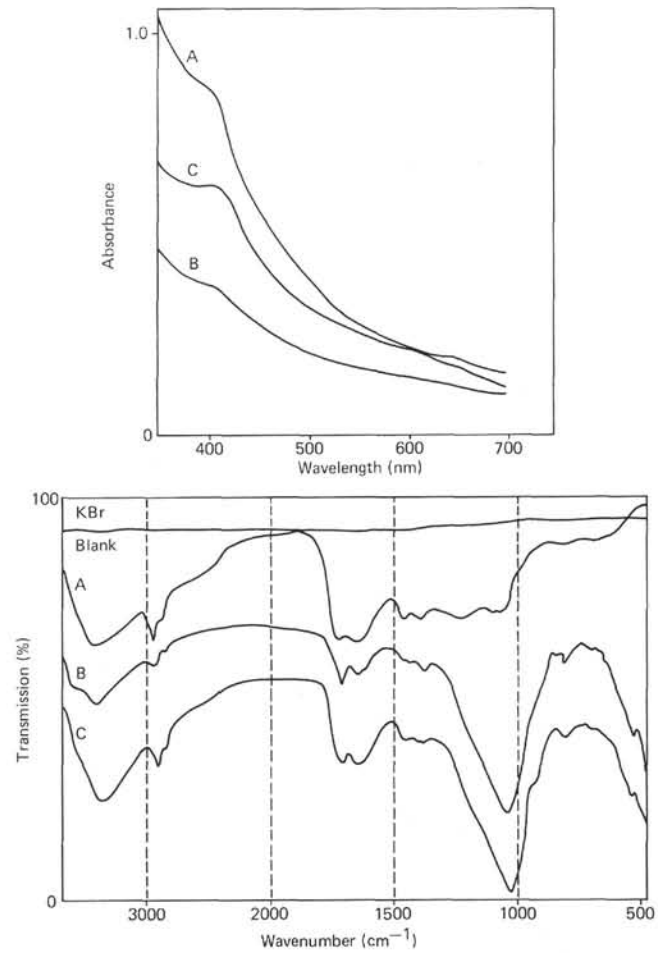

Figure 13. *Visible and infrared spectra of humic acids.* A. *Section 440A-7-6;* B. *Section 440B-68-2;* C. *Section 436-11-4.*

Si-O bonds (e.g., 1040, 800cm^{-1}) (Figure 12). All spectra show major absorptions due to saturated C-H bonds, C=C bonds, C=O bonds, and OH bonds in their various environments. Other forms of C to O bond are also present (phenoxy C-O, methoxy, aromatic/aliphatic C-O-C). Broad, weak bands possibly corresponding to aromatic substitution patterns are present (Flaig et al., 1975; Huc et al., 1978). Nitrogen contents are high, but there is no evidence of high 1540cm^{-1} amide absorption, though absorptions due to amines and heterocyclic-N would be contributing to the spectra.

The HAs from Sections 440A-7-6 and 436-11-4 are very similar in their IR absorptions. Section 440B-68-2 has a considerably different spectrum than the shallower sample (Section 440A-7-6), with the intensities of both aliphatic/aromatic C-H and C=C bond absorptions being reduced relative to that of C=O.

Carotenoids

Carotenoids were assigned from their uv/vis spectra recorded by stopped-flow scanning in HPLC analysis. Assignments were confirmed by HPLC coinjection with authentic standards. The series of samples from Site 440 show a quantitative decrease (Table 18) of carotenoids

TABLE 18
Carotenoid Concentrations (ng/g dry sediment; saponified samples)

	Structure[a]	Section 440A-7-6	440B-3-5	440B-8-4	436-11-4
β-carotene	XLI	130	120	2.8	2.2
Diatoxanthin	XLII	65	34	n.d.	n.d.
Other		80	53	n.d.	n.d.

Note: For explanation of n.d. see Note to Table 3.
[a]See Appendix, this chapter.

with depth and preferential degradation of the xanthophylls (Table 18). The shallower two samples (Sections 440A-7-6 and 440B-3-5) showed three main carotenoids, tentatively identified as β-carotene, diatoxanthin, and an unidentified polar xanthophyll. Section 440B-8-4 shows only one carotene, tentatively identified as β-carotene, with a concentration about 3 per cent of that of β-carotene in the upper samples. Section 440B-68-2 contains no measurable amounts of carotenoids.

The sample analyzed from the eastern side of the Japan Trench (Section 436-11-4) contained very low quantities of pigments, which precluded detailed analysis.

GEOLOGICAL DATA

An attempt to rationalize the lipid distribution should be made in the light of the geological data from the site summaries (this volume, Pt. 1). Smear slide data in particular have proved useful.

Environmental Setting

The samples were chosen to span a range of compositional, spatial, and chronological criteria for comparison with the lipid distribution patterns. The ages of the five samples selected are given in Table 1. The Site 436 sample is positioned on the outer slope of the Japan Trench (i.e., on the ocean side), where terrestrial flux from Japan should be low. In contrast, Site 440 samples are located closer to Japan on the inner slope. All samples were deposited at or below the carbonate compensation depth. In terms of the present day, the water depth at Site 436 is approximately 6 km, whereas that of Site 440 is 5 km. On the basis of assemblages of benthonic foraminifers, the paleodepth for the five samples is tentatively placed below 2 km; displaced faunas complicate this assignment, however. The presence of indigenous benthic foraminifers and abundant sponge spicules in all the samples (or adjacent sections) implies that sufficient oxygen was present for the development of an invertebrate fauna. In particular, the sediment at Site 436 must have been oxic, because the presence of fecal pellets implies the activity of benthic arthropods.

Input

Data for the five samples have been grouped into marine, terrestrial, and other components (Tables 19A and 19B). The marine component is greatest in Section 436-11-5 (21 per cent) and adjacent sections, which contain a high proportion of diatoms (15 per cent). The Site 440 sections show a lower proportion of marine debris (8–18 per cent), which decreases from the youngest (lower Pleistocene) to the oldest (upper Miocene) samples.

The terrestrial component is lower at Site 436 (58 per cent) than in the Site 440 samples (65–72 per cent). In particular, the presence of quartz grains and heavy minerals in the latter implies the action of high-energy transportation mechanisms from the Japanese mainland. The inorganic diagenetic component is represented mainly by pyrite. This mineral is present (0–2 per cent) in two Site 440 samples, but samples adjacent to the Site 436 section contain only trace amounts.

Other mineral components present in the sediments are volcanic debris (18–20 per cent), found in all sections, and a lower proportion of unspecified carbonate (< 10 per cent).

In general, the depositional characteristics are those of a deep-water marine facies dominated by terrestrial input derived from a nearby landmass. A major interest for organic geochemistry is to investigate evidence of a highly productive ancient water column.

The increasing proportion of the marine component as one proceeds up the sedimentary column (i.e., from the oldest Site 440 sample considered here to the youngest) may be reflected in the increase in organic carbon values.

The Site 436 sample is an exception to these trends in that its marine component is higher than all those of these Site 440 sections, yet its organic carbon content is only 0.4 per cent.

Sediment Accumulation Rate

The anomalously low organic carbon content of Site 436 may be rationalized in terms of the low sediment accumulation rate of this site. This comparatively low rate would give benthic bacteria more time to degrade the organic components into CO_2, leaving only the most resistant organic matter. In contrast, Site 440 has a much higher sediment accumulation rate, possibly leading to a better preservation of the various organic components. It is not yet possible to decide whether the increase in organic carbon at Site 440 is due to an increasing sedimentation rate through time, to an input change (i.e., proportion of marine detritus), or to a combination of these factors. Biological diagenesis may also be responsible for diminution of organic carbon with depth.

Diagenesis and Physicochemical Parameters

The high alkalinities present at Site 440 probably indicate bacterial oxidation of various organic molecules via sulphate reduction. The highest alkalinities are found in the topmost sample and diminish with depth. The alkalinity pattern is very similar to that of the organic carbon values, implying a correlation between organic carbon values and bacterial activity. The high biogenic gas content further confirms this view. Site 436 shows low organic carbon and alkalinity values and, as would be expected, contains no biogenic gas. This observation implies that the activity of sulphate-reducing bacteria may have been virtually complete here following initial sediment burial. The very low thermal flux at

TABLE 19A
Input and Depositional Characteristics of Relevant Sections[a]

	Section					
	440A-7-7	440B-3-5	440B-8-5	440B-68-2	436-11-5	Remarks
Marine Input (%)						
Glauconite	1	–	1	1	–	Progressive dimunition of marine component downhole at Site 440. High marine input Site 436.
Diatoms	12	13	5	4	15	
Radiolaria	2	1	Tr	–	1	
Sponge spicules	3	3	4	3	5	
Total	18	17	10	8	21	
Terrestrial Input (%)						
Heavy minerals	1	2	1	3	–	Lower terrestrial input at Site 436. Clays may also be derived from altered volcanics.
Clay	55	57	43	42	58	
Quartz	9	8	28	23	–	
Total	65	67	72	68	58	
Other Volcanic Diagenetic (%)						
Carbonate	9	8	1	–	–	Most feldspar probably derived from vitric tuffs, i.e. volcanically.
Volcanics	2	4	9	14	15	
Feldspar	5	4	6	10	5	
Pyrite	1	–	2	–	Tr	
Total	17	16	18	24	20	
General depositional characteristics of the area	High productivity area (dominated by diatom input superimposed upon considerable terrestrial input).			Represents somewhat lower productivity than younger samples.	Lower productivity area than Site 440 (% figures misleading).	Much slumping and sediment displacement downslope for Site 440.
Depositional rate (cm/1000 yrs)	General increase of sedimentation rate through time.					Rate of sedimentation at Site 436 is four times lower than Site 440.
	23	23	14	10	5	
Relationships between productivity sedimentation rate and organic carbon	The high sedimentation rates and productivity at this site have meant that the sediment is highly reducing, i.e., $SO_4^{=}$ reduced to $S^{=}$, CO_2, CH_4. Good preservation of marine and terrestrial organic matter.				The lower sedimentation rate and productivity mean more oxidizing sediment. Less $SO_4^{=}$ reduction, CH_4 generation, and lipid preservation expected.	Site 436 and Site 440 deposited in different facies.

Note: For explanation of Tr see Note to Table 3.
[a]See Site Summaries, this volume, Pt. 1.

TABLE 19B
Physical and Chemical Properties of Diagenetic Interest[a]

	Section					
	440A-7-6	440B-3-5	440B-8-4	440B-68-2	436-11-4	Remarks
Porosity	70	60	60	58	73	Gradual diminution in water content with depth. Porosities remain high.
Water Content (%)	44	35	34	30	55	
Alkalinity (m.eq/l)	90	73	70	10	10	Reflects bacterial bicarbonate ion generation (sulphate-reducing bacteria).
Gaseous Hydrocarbon (%)	82.3 CH_4 and $C_2 \rightarrow C_5$ Hydrocarbon gas.	86.5 CH_4	68 CH_4	57.7 CH_4	None also no H_2S present.	Absolute CH_4 values not given.
		Gradual increase downhole (of biogenic origin).				
Downhole Temperature	All temperatures lower than surface waters (15.5°C) 10°C increase in temperature per kilometer.				Not given but must be near temperature of adjacent seawater.	–

[a]See Site Summaries, this volume, Pt. 1.

Site 440 (<10 °C/km) implies that the extent of thermal maturation would be low.

A wide range of lipid parameters demonstrates the immaturity of the organic matter of the Japan Trench samples, which is in agreement with the low geothermal gradient. These include (1) dominance of functionalized components over their saturated counterparts (e.g., *n*-alcohols over *n*-alkanes, sterols over steranes, etc.); (2) retention of high carbon preference indices for straight-chain components; (3) preservation of unsatu-

rated components, even in the deepest sample (440B-68-2); and (4) dominance of 17βH-hopanes over their 17αH counterparts.

CONCLUSIONS AND SUMMARY

The lipids of the Japan Trench samples originate from three different sources: terrestrial, marine, and bacterial. The key components or distributions indicative of these inputs in this context are summarized as follows:

Terrestrial Indicators

1) *n*-alkane, *n*-methyl ketone, *n*-alkanol, and *n*-alkenol distributions;
2) the presence of 3-oxytriterpenoids and their aromatic derivatives;
3) the recognition of fern-9(11)-ene;
4) the presence of relatively high quantities of 24-ethylcholest-5-en-3β-ol and 24-ethyl-5α-cholestan-3β-ol in the sterols (Site 440 samples only);
5) the presence of aromatic diterpenoids, retene, and simonellite;
6) the dominance of 9,16 di-OH hexadecanoic acid over the 10,16 isomer.

Marine Indicators (nonbacterial)

1) marine sterols, i.e., C_{26} and C_{30} sterols, 23,24-dimethylsterols, $\Delta^{24(28)}$ sterols, etc.;
2) very long chain ketones and ethers indicative of coccolithophore inputs (skeletal debris are absent below carbonate compensation depth);
3) sterol ethers;
4) high amounts of phytol;
5) the diatom carotenoid, diatoxanthin.

Bacterial Indicators

1) The similarity of *n*-alkane and *n*-methylketone distributions;
2) the presence of extended hopanoids, i.e., acids, alcohols, ketones, alkanes, etc.;
3) the presence of steroidal ketones;
4) the presence of aromatic components derived from 3-oxytriterpenoids;
5) the presence of squalane;
6) the presence of β-OH acids tentatively assigned to *Desulphovibrio* genus.

The four samples at Site 440 provide indications of diagenetic transformations illustrating their increasing maturity with depth. Various parameters show this trend, and the principal ratios that increase with depth are as follows:

1) Diasterene/Δ^2 sterene;
2) sterane/sterene;
3) hop-17(21)-ene/hop-22(29)-ene;
4) 17αH, 21βH/17βH, 21βH for hopane and homohopane;
5) retene/simonellite;
6) phytane/phytenes;
7) phytane/phytol;
8) pristane/phytol.

The top two samples (Sections 440A-7-6 and 440B-3-5), which are only 27 meters apart in depth, show great similarities in the distributions and quantities of most of their lipid components. These likenesses illustrate the reproducibility of the organic geochemical results from different samples of similar lithologies and ages.

In addition to the diagenetic trend at Site 440, the lipid distributions indicate that the level of productivity was lower, and/or the water column more oxic, during deposition of Sections 440B-8-4 and 440B-68-2 than for the shallower samples. Such indicators are the lower relative amounts in the deeper samples of the following:

1) Sterols and their diagenetic products, stanols, sterenes, sterones, diasterenes, etc.;
2) acyclic diterpenoids, i.e., phytol and its diagenetic products, phytenes, phytane, pristane, and 6,10,14-trimethylpentadecan-2-one;
3) very long chain ketones;
4) sterol ethers.

The lipid distributions of Section 436-11-4 differ from those of the Site 440 samples in the following respects:

1) The abundance of sterols, and hence their diagenetic products sterenes, diasterenes, steranes, etc., is markedly lower.
2) The amounts of phytol and its diagenetic products are markedly lower.
3) The methyl/ethyl ratio of the very long chain ketones is greater, suggesting a different source of organism.
4) Branched alkanols are absent.

The main similarities are the following:

1) The sterol ethers present;
2) the distributions of *n*-alkanes, *n*-methyl ketones, *n*-alkanols, and *n*-alkenols;
3) the range of hopanes and hopenes present.

These results augment and are an extension of the geological data, which show a greatly reduced proportion of marine input in Sections 440B-8-5 and 440B-68-2 (Table 19A).

The differences between the Site 440 samples and Section 436-11-4 can be attributed largely to lower productivity in the water column. The terrestrial input to Section 436-11-4 is lower (absolutely) than for the Site 440 samples but is more easily discerned because the marine input to Section 436-11-4 is also low and hence does not mask the terrestrial component so effectively. These deductions may again be used to complement the geological data of Tables 19A and 19B. The measurements specific to organic geochemistry can provide information unobtainable by other geologic disciplines — for instance, the assessment here of marine input from coccolith-derived long-chain ketones. On the other hand, the lability of particular marine lipids, e.g., many carotenoids, causes their sedimentary distributions to be partially unrepresentative of the original lipid inputs and inevitably introduces some uncertainty into conclusions concerning the depositional environment.

Some description of the samples may also be obtained by grouping the quantitated components according to structural characteristics (Table 20). This procedure at-

TABLE 20
Structural Components (ng/g dry sediment)

Component	Section 440A-7-6	440B-3-5	440B-8-4	440B-68-2	436-11-4
nC_9-nC_{20} straight-chain (short)	254	326	132	178	103
nC_{21}-nC_{35} straight-chain (long)	1207	1383	259	377	173
nC_{36}-nC_{40} straight-chain (very long)	715	719	126	38	243
nC_{10}-nC_{20} branched-chain (short)	17.3	7.4	3.2	0.5	0.1
nC_{21}-nC_{35} branched-chain (long)	41.3	54	18	9.5	n.d.
Acyclic isoprenoid	191	191	21	5	1
Cyclic diterpenoid	17	14	9	9	8
Steroidal	461	344	63	117	6
Hopanoidal	58	74	12	14	8
Other triterpenoids	35	29	12	18	6
Nonterpenoid PAHs	141	65	66	70	31
Carotenoids	275	208	28	n.d.	2

Note: For explanation of n.d. see Note to Table 3.

tempts to minimize the effects of diagenetic processes by considering the carbon skeleton of related compounds. Two results in particular are of interest. Short-chain (n-C_{10}–n-C_{20}) material such as alkanes, alkanols, alkenols, fatty acids, etc., may be grouped to estimate a marine input from algae, bacteria, etc. An overall decrease occurs downhole, which may be compared with the diminution of algal components of nearby sections on micropaleontological criteria (Table 19A). Terrestrial markers (higher plant lipids) include the longer chain (n-C_{21}–n-C_{35}) components. This summed component is much higher in the top two Site 440 samples than in any others. The value for Section 436-11-4 is particularly low. These values may be contrasted with the relatively insensitive visual estimates of Table 19A.

All these results may be compared with those of other selected sediments. The major similarities between Site 440 samples and sediments from Walvis Bay (Wardroper et al., 1978; Wardroper, 1978) or Walvis Ridge (Boon et al., 1978; Boon and de Leeuw, 1979) are the following:

1) The presence of complex marine sterol distributions, very long chain ketones, C_{15} iso- and anteiso-alcohols, sterol ethers, and fernenes;

2) the abundances of phytol, phytenes, 2,6,10,15,19-pentamethyleicosane, and 6,10,14-trimethylpentadecan-2-one.

Major differences occur in the following:

1) The presence of n-C_{16} as the major n-alkanol of Walvis Bay;

2) the dominance of n-C_{17} in the n-alkanes of Walvis Bay;

3) The absence of squalane in Walvis Bay.

The similarities reflect the common marine input to both high productivity areas, and the differences may arise from the higher marine to terrestrial proportion of input to Walvis Bay. Walvis Ridge, however, does possess a terrigenous input, as indicated by its n-alkane distribution and the presence of fernene (Boon et al., 1978). The geological data for Walvis Ridge (Bolli, Ryan, et al., 1978) show that general similarities exist between the depositional environments of this area and the Japan Trench. In particular, productivity (as seen in diatom input) was high in both during the late Miocene, Pliocene, and Pleistocene. However, Walvis Ridge sediments contain much more carbonate than the Japan Trench sediments, which were deposited near and below the carbonate compensation depth. The smaller amounts of lower carbon number straight-chain components in the Japan Trench, compared to Walvis Bay, can be explained by their dilution by terrestrial inputs or their preferential degradation relative to higher carbon numbers, or a combination of the two.

When the same compound classes have been examined in both, the Japan Trench lipid distributions also resemble those of sediments from the Blake-Bahama Basin (Cardoso et al., 1978; Wardroper, 1979), except in the absence of diasterenes in the latter. The similarities reflect a mixed marine and terrigenous input to both suites of samples.

Ancient sediments from the Bay of Biscay continental slope (Barnes et al., 1979; Wardroper, 1979) and the northwestern African continental margin (Brassell et al., in press, and unpublished data) also show major similarities to these samples in diasterenes and 4-methyldiasterenes, hopenes, n-alkanes (Leg 50 samples only), perylene, steranes, monoaromatic steroids (Leg 50 samples only), and hopanoid ketones.

The striking resemblance in the diasterene distribution of Legs 48, 50, and 57 samples suggests that the diagenetic transformations in the samples are broadly similar. Many of these processes begin from a limited number of components (e.g., diasterenes from Δ^2 sterenes). A major difference, apart from those attributable to the different sample maturities, is that the n-alkane and n-methyl ketone distributions are dissimilar in the Leg 48 samples and virtually identical in those from the Japan Trench. Also, 2,6,10,15,19-pentamethyleicosane and squalane are present only in the latter, and the n-alkanol distributions of Leg 48 and Legs 56/57 samples show major differences.

It appears, therefore, that although the diagenetic processes operating in the three environments are similar, the inputs to each suite of samples differ principally in the proportion of marine components.

The features of the Japan Trench samples shown by organic geochemical analysis can be summarized as follows:

1) immaturity of the samples;

2) a major difference in input across the trench;

3) a higher proportion of autochthonous components on the western trench slope compared to the distal side, which is also greater in the lower Pleistocene than in the Miocene;

4) a gradual diagenetic transformation of lipids at Site 440 as the sample depth increases;

5) several similarities to another present-day area of high productivity (Walvis Bay);

6) diagenetic processes similar to those found in Cretaceous sediments from the Atlantic.

ACKNOWLEDGMENTS

We thank the Natural Environment Research Council (GR3/2951 and supplement; GR3/3758 data acquisition) for support. J. M. and S. C. B. acknowledge Research Studentships from the Natural Environment Research Council, as does I. D. T. from the Science Research Council. J. K. V. acknowledges support from the Natural Environment Re-

search Council (GR3/3419). We thank Mrs. A. P. Gowar for assistance with GC–MS analyses. We also thank Mr. G. Cooles of British Petroleum Ltd., Research Division (Sunbury-on-Thames) for subsample analyses and C. Cornford and D. Leythaeuser for helpful criticism.

REFERENCES

Barnes, P. J., Brassell, S. C., Comet, P. A., Eglinton, G., McEvoy, J., Maxwell, J. R., Wardroper, A. M. K., and Volkman, J. K., 1979. Preliminary lipid analyses of core sections 18, 24, and 30 from Hole 402A. *In* Montadert, L., Roberts, D. G., et al., *Init. Repts. DSDP,* 48: Washington (U.S. Govt. Printing Office), 965–976.

Bolli, H. M., Ryan, W. B. F., et al., 1978. Walvis Ridge–Sites 362 and 363. *In* Bolli, H. M., Ryan, W. B. F., et al., *Init. Repts. DSDP,* 40: Washington (U.S. Govt. Printing Office), 183–263.

Boon, J. J., and de Leeuw, J. W., 1979. The analysis of wax esters, very long mid-chain ketones and sterol ethers isolated from Walvis Bay diatomaceous ooze. *Mar. Chem.,* 7, 117–132.

Boon, J. J., van der Meer, F. W., Schuyl, P. J. W., de Leeuw J. W., Schenck, P. A., and Burlingame, A. L., 1978. Organic geochemical analyses of core samples from Site 362, Walvis Ridge, DSDP Leg 40. *In* Bolli, H., Ryan, W. B. F., et al., *Init. Repts. DSDP,* Suppl. to Vols. 38, 39, 40, and 41: Washington (U.S. Govt. Printing Office), 627–637.

Brassell, S. C., Comet, P. A., Eglinton, G., McEvoy, J., Maxwell, J. R., Quirke, J. M. E, and Volkman, J. K., in press. Preliminary lipid analysis of core sections 14, 18, and 28 from Hole 416A. *In* Lancelot, Y., Winterer, E. L., et al., *Init. Repts. DSDP,* 50: Washington (U.S. Govt. Printing Office).

Cardoso, J. N., Wardroper, A. M. K., Watts, C. D., Barnes, P. J., Maxwell, J. R., Eglinton, G., Mound, D. G., and Speers, G. C., 1978. Preliminary organic geochemical analyses; Site 391, Leg 44 of the Deep Sea Drilling Project. *In* Benson, W. E., Sheridan, R. E., et al., *Init. Repts. DSDP,* 44: Washington (U.S. Govt. Printing Office), 617–623.

Flaig, W., Beutelspacher, H., and Rietz, H., 1975. Chemical composition and physical properties of humic substances. *In* Gieseking, J. E. (Ed.), *Soil Components* (Vol. 1): New York (Springer-Verlag), 1–187.

Huc, A. Y., Durand, B., and Monin, J. C., 1978. Humic compounds and kerogens in cores from Black Sea sediments, Leg 42B, Holes 379A, B and 380A. *In* Ross, D. A., Neprochnov, Y. P., et al., *Init. Repts. DSDP,* 42, Pt. 2: Washington (U.S. Govt. Printing Office), 737–748.

Philp, R. P., Brown, S., Calvin, M., Brassell, S., and Eglinton G., 1978. Hydrocarbon and fatty acid distributions in recently deposited algal mats at Laguna Guerrero, Baja California. *In* Krumbein, W. E. (Ed.), *Environmental Biogeochemistry and Geomicrobiology* (Vol. 1: *The Aquatic Environment*): Ann Arbor (Ann Arbor Science), 255–270.

Spyckerelle, C., 1975. Constituants aromatiques de sediments [Ph.D. dissert.] Université Louis Pasteur, Strasbourg, France.

Spyckerelle, C., Greiner, A. Ch., Albrecht, P., and Ourisson, G., 1977a. Aromatic hydrocarbons from geological sources III. A tetrahydrochrysene derived from triterpenes in Recent and old sediments, 3,3,7-bismethyl-1,2,3,4,-tetrahydrochrysene. *J. Chem. Res.* (M), 3746–3777 (S), 330–331.

_____, 1977b. Aromatic hydrocarbons from geological sources IV. An octahydrochrysene, derived from triterpenes in Recent and old sediments, 3,3,7,12a-tetramethyl-1,2,3,4, 4a,11,12,12a-octahydrochrysene. *J. Chem. Res.* (M), 3801–3828 (S), 332–333.

Streibl, M., and Herout, V., 1969. Terpenoids—especially oxygenated mono-, sesqui-, di- and triterpenes. *In* Eglinton, G., and Murphy, M. T. J. (Eds.), *Organic Geochemistry, Methods and Results:* Heidelberg (Springer-Verlag), pp. 401–424.

Volkman, J. K., Eglinton, G., Corner, E. D. S., and Sargent, J. R., in press. Novel unsaturated straight chain C_{37}-C_{39} methyl and ethyl ketones in marine sediments and a coccolithophore *Emiliania huxleyi. In* Douglas A. G., and Maxwell, J. R. (Eds.), *Advances in Organic Geochemistry 1979:* Oxford (Pergamon Press).

Wardroper, A. M. K., 1979. Aspects of the geochemistry of polycyclic isoprenoids [Ph.D. dissert.]. University of Bristol, U. K.

Wardroper, A. M. K., Maxwell, J. R., and Morris, R. J., 1978. Sterols of a diatomaceous ooze from Walvis Bay. *Steroids,* 32, 203–221.

APPENDIX

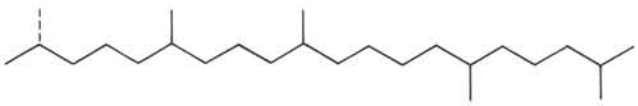

I

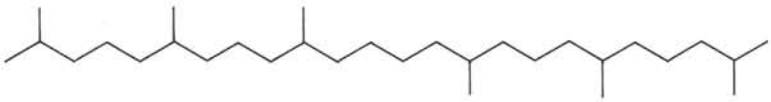

II

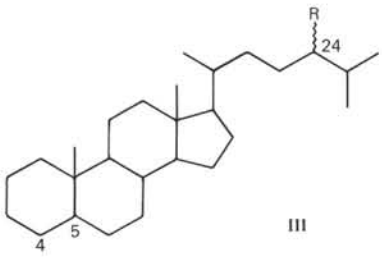

III

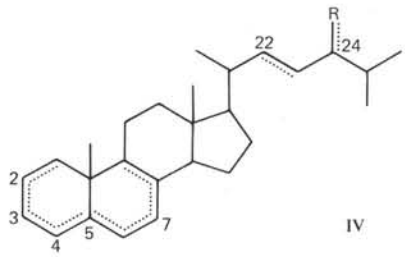

IV

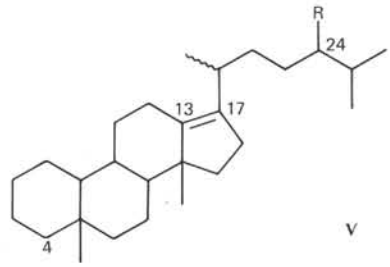

V

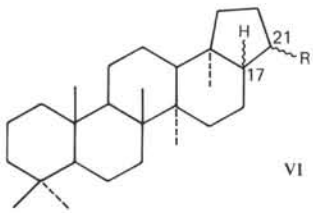

VI

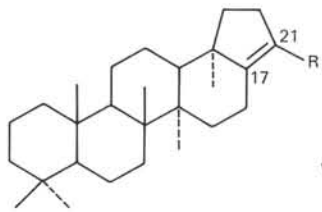

VII

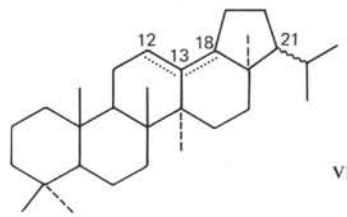

VIII

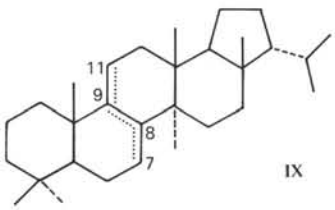

IX

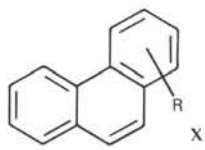

X

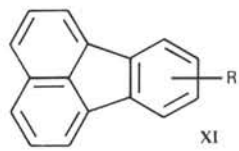

XI

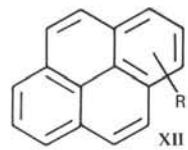

XII

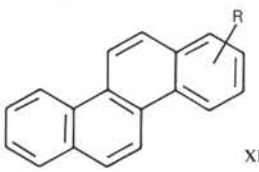

XIII

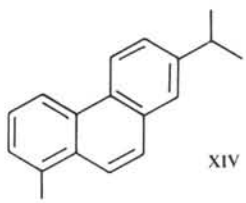

XIV

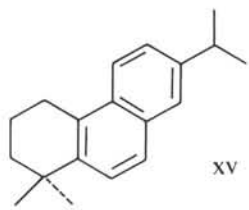

XV

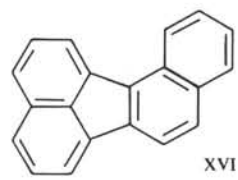

XVI

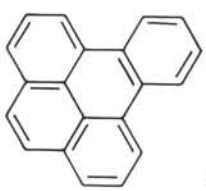

XVII

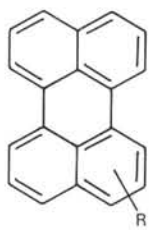

XVIII

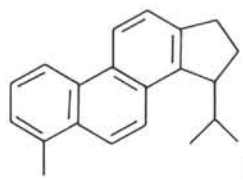

XIX

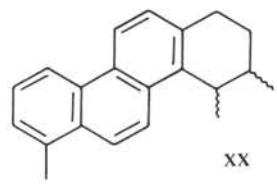

XX

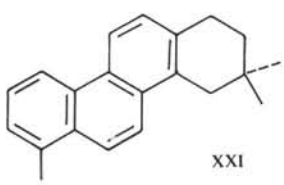

XXI

XXII

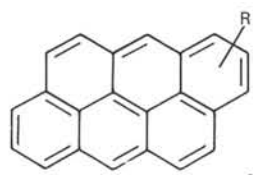

XXIII

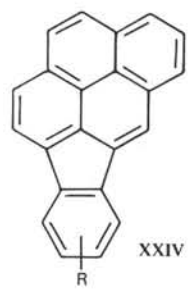

XXIV

APPENDIX – *Continued*

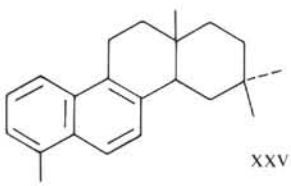
XXV

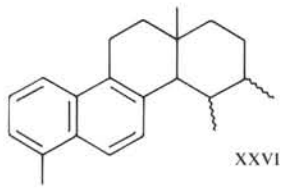
XXVI

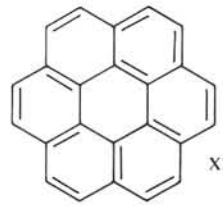
XXVII

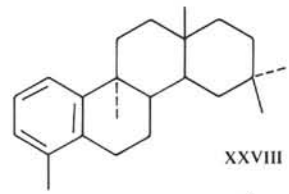
XXVIII

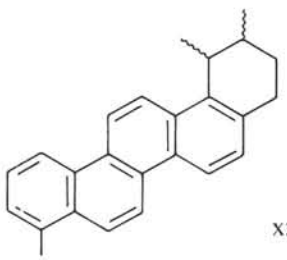
XXIX

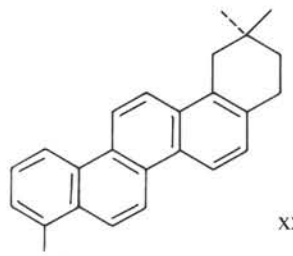
XXX

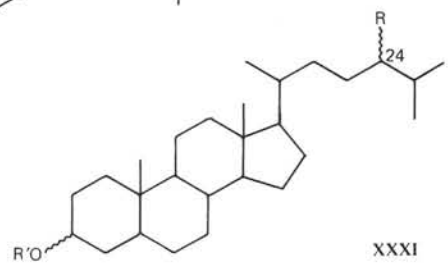

XXXI

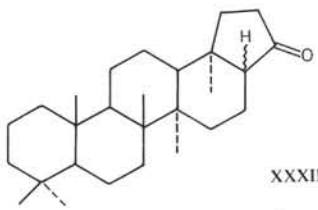

XXXII

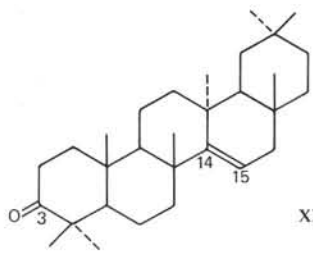

XXXIII

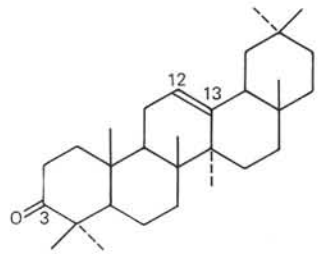

XXXIV

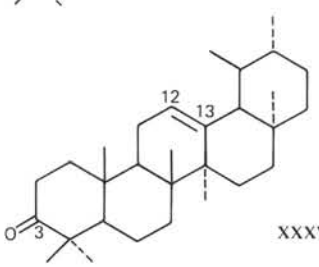

XXXV

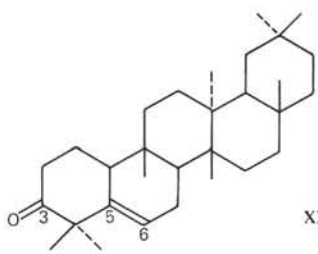

XXXVI

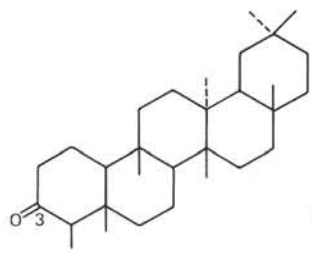

XXXVII

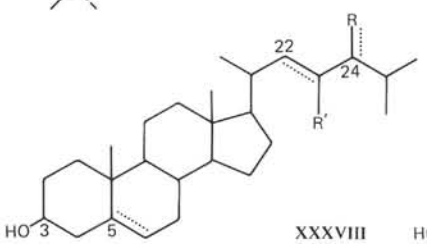

XXXVIII

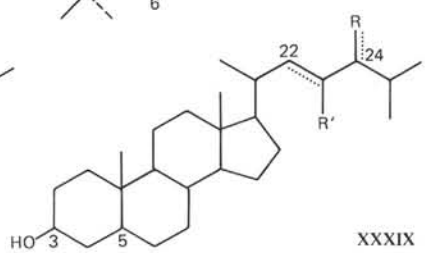

XXXIX

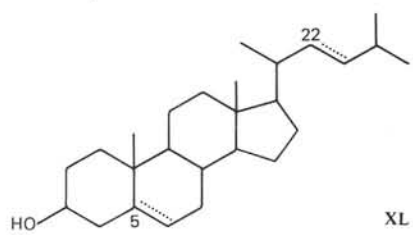

XL

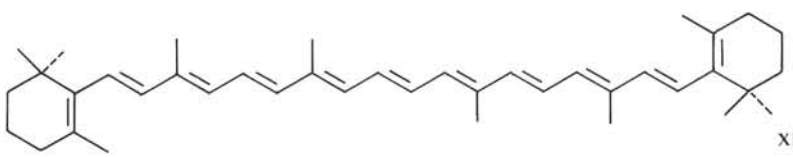
XLI

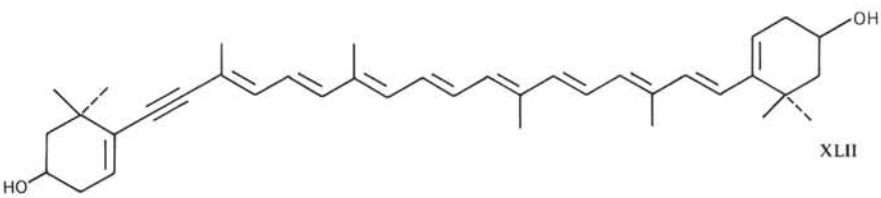

XLII